Vibration Analysis of Cracked beam

A Thesis Submitted in partial fulfillment
of the requirements for the award of

Master of Technology
In

Machine Design and Analysis

By

Mogal Shyam Prabhakar
Roll No: 207ME114

Department of Mechanical Engineering
National Institute of Technology
Rourkela
2009

Vibration Analysis of Cracked beam

A Thesis Submitted in partial fulfillment
of the requirements for the award of

Master of Technology
In

Machine Design and Analysis

By

Mogal Shyam Prabhakar
Roll No: 207ME114

Under the Guidance of

Dr. R. K. BEHERA

Department of Mechanical Engineering
National Institute of Technology
Rourkela
2009

National Institute of Technology
Rourkela

CERTIFICATE

This is to certify that the thesis entitled, **"Vibration Analysis of Cracked beam"** submitted by **Mr. Mogal Shyam Prabhakar** in partial fulfillment of the requirements for the award of Master of Technology Degree in **Mechanical Engineering** with specialization in **"Machine Design and Analysis"** at the National Institute of Technology, Rourkela is an authentic work carried out by him under my supervision and guidance.

To the best of my knowledge, the matter embodied in the thesis has not been submitted to any other University / Institute for the award of any Degree or Diploma.

Date: 26/05/2009

Dr. R. K. Behera
Department of Mechanical Engineering
National Institute of Technology
Rourkela-769008

ACKNOWLEDGEMENT

Successful completion of work will never be one man's task. It requires hard work in right direction. There are many who have helped to make my experience as a student a rewarding one.

In particular, I express my gratitude and deep regards to my thesis guide **Prof. R. K. Behera** first for his valuable guidance, constant encouragement and kind co-operation throughout period of work which has been instrumental in the success of thesis.

I also express my sincere gratitude to **Prof. R. K. Sahoo**, Head of the Department, Mechanical Engineering, for providing valuable departmental facilities.

I would like to thank my fellow post-graduate students.

Mogal Shyam Prabhakar
Roll No. 207ME114
Department of Mechanical Engg
National Institute of Technology
Rourkela

CONTENTS

ABSTRACT

Cracks in vibrating component can initiate catastrophic failures. The presences of cracks change the physical characteristics of a structure which in turn alter its dynamic response characteristics. Therefore there is need to understand dynamics of cracked structures. Crack depth and location are the main parameters for the vibration analysis. So it becomes very important to monitor the changes in the response parameters of the structure to access structural integrity, performance and safety. To examine the effect of the crack to the natural frequency of beams.

In the present study, vibration analysis is carried out on a cantilever beam with two open transverse cracks, to study the response characteristics. In first phase local compliance matrices of different degree of freedom have been used model transverse cracks in beam on available expression of stress intensity factors and the associated expressions for strain energy release rates. Suitable boundary condition are used to find out natural frequency and mode shapes. The results obtained numerically are validated with the results obtained from the simulation. The simulations have done with the help of ANSYS software.

A neural network for the cracked structure is trained to approximate the response of the structure by the data set prepared for various crack sizes and locations. Feed-forward multi-layer neural networks trained by back-propagation are used to learn the input (the location and depth of a crack)-output (the structural eigenfrequencies) relation of the structural system. With this trained neural network minimizing the difference from the measured frequencies.

It is verified from both computational and simulation analysis that the presence of crack decreases the natural frequency of vibration. The mode shapes also changes considerably due to the presence of crack.

List of Tables

List of Figures

Nomenclature

a_1 = Crack depth

a_2 = Crack depth

A, i=1,18=Unknown co-efficients of matrix A

B= Width of beam

$C_u = \left(E/\rho\right)^{1/2}$

$C_y = (EI/\mu)^{1/2}$

E = Young's Modulus of elasticity

I = Section Moment of Inertia of beam

ρ = density

υ= Poisson's ratio

J= Strain energy release rate

$\bar{k}_u = \omega L/C_u$

$\bar{k}_y = (\omega L^2/C_y)^{1/2}$

K_I,i=1,2=Stress intensity factor for P_i loads

K_{ij} =Local flexibility matrix element

$K^{'}$,$K^{"}$= Stiffness matrix of first and second crack location

$\left|Q\right|$=determinant of Q

w= depth of beam

$\beta = L_1/L$

$\gamma = L_2/L$

$\mu = A\rho$

y(n) = output of the neuron

μ = convergence coefficient

CHAPTER 1

INTRODUCTION

1. INTRODUCTION

It is required that structures must safely work during its service life. But, damages initiate a breakdown period on the structures. Cracks are among the most encountered damage types in the structures. Cracks in a structure may be hazardous due to static or dynamic loadings, so that crack detection plays an important role for structural health monitoring applications. Beam type structures are being commonly used in steel construction and machinery industries. In the literature, several studies deal with the structural safety of beams, especially, crack detection by structural health monitoring. Studies based on structural health monitoring for crack detection deal with change in natural frequencies and mode shapes of the beam.

The most common structural defect is the existence of a crack. Cracks are present in structures due to various reasons. The presence of a crack could not only cause a local variation in the stiffness but it could affect the mechanical behavior of the entire structure to a considerable extent. Cracks may be caused by fatigue under service conditions as a result of the limited fatigue strength. They may also occur due to mechanical defects. Another group of cracks are initiated during the manufacturing processes. Generally they are small in sizes. Such small cracks are known to propagate due to fluctuating stress conditions. If these propagating cracks remain undetected and reach their critical size, then a sudden structural failure may occur. Hence it is possible to use natural frequency measurements to detect cracks.

In the present investigation a number of literatures published so far have been surveyed, reviewed and analysed. Most of researchers studied the effect of single crack on the dynamics of structures. However in actual practice structural members such as beams are highly susceptible to transverse cross-sectional cracks due to fatigue. Therefore to attempt has been made to investigate the dynamic behavior of basic structures with crack systematically.

The objective is to carry out vibration analysis on a cantilever beam with and without crack. The results obtained analytically are validated with the simulation results. In first phase of the work two transverse surface cracks are included in developing the analytical expressions in dynamic characteristics of structures. These cracks introduce new boundary

conditions for the structures at the crack locations. These boundary conditions are derived from strain energy equation using castiligiano's theorem. Presence of crack also reduces stiffness of the structures which has been derived from stiffness matrix. The detailed analyses of crack modeling and stiffness matrices are presented in subsequent sections.

Euler-Bernoulli beam theory is used for dynamic characteristics of beams with transverse cracks. Modified boundary conditions due to presence of crack have been used to find out the theoretical expressions for natural frequencies and mode shape for the beams.

The use of neural networks in detecting the damage has been developed for several years, because of their ability to cope with the analysis of the structural damage without the necessity for intensive computation. Recently, neural networks are expected to be a necessity for intensive computation. Recently, neural networks are expected to be a potential approach to detect the damage of the structure. In this study feed-forward multi-layer neural networks trained by back-propagation are used to learn the input (the location and depth of a crack)-output (the structural eigenfrequencies) relation of the structural system. A neural network for the cracked structure is trained to approximate the response of the structure by the data set prepared for various crack sizes and locations.

CHAPTER 2

LITERATURE REVIEW

2. LITERATURE REVIEW

When a structure suffers from damages, its dynamic properties can change, especially, crack damage can cause a stiffness reduction, with an inherent reduction in natural frequencies, an increase in modal damping, and a change of the mode shapes. For vibration analysis of cracked beams and possible crack detection, the fracture mechanics procedure is generally preferred. According to this procedure the crack occurring in a beam would reduce the local stiffness at the location of crack. In using the fracture mechanics model, the local stiffness at the crack section is calculated using Castigliano's second theorem as applicable to fracture mechanics formulations. The calculated local stiffness is then modeled by a flexural spring for the bending vibration of a cracked beam. To establish the vibration equations, the cracked is represented by two structures connected by flexural spring.

Orhan Sadettin [1] has studied the free and forced vibration analysis of a cracked beam was performed in order to identify the crack in a cantilever beam. Single- and two-edge cracks were evaluated. Dynamic response of the forced vibration better describes changes in crack depth and location than the free vibration in which the difference between natural frequencies corresponding to a change in crack depth and location only is a minor effect.

Chasalevris and Papadopoulos [2] have studied the dynamic behaviour of a cracked beam with two transverse surface cracks. Each crack is characterised by its depth, position and relative angle. A local compliance matrix of two degrees of freedom, bending in the horizontal and the vertical planes is used to model the rotating transverse crack in the shaft and is calculated based on the available expressions of the stress intensity factors and the associated expressions for the strain energy release rates.

Nahvi and Jabbari [3] have developed an analytical, as well as experimental approach to the crack detection in cantilever beams by vibration analysis. An experimental setup is designed in which a cracked cantilever beam is excited by a hammer and the response is obtained using an accelerometer attached to the beam. To avoid non-linearity, it is assumed that the

crack is always open. To identify the crack, contours of the normalized frequency in terms of the normalized crack depth and location are plotted.

Yang et al.[4] have developed an energy-based numerical model is to investigate the influence of cracks on structural dynamic characteristics during the vibration of a beam with open crack. Upon the determination of strain energy in the cracked beam, the equivalent bending stiffness over the beam length is computed.

Dharmaraju et al.[5] have used Euler–Bernoulli beam element in the finite element modeling. The transverse surface crack is considered to remain open. The crack has been modeled by a local compliance matrix of four degrees of freedom. This compliance matrix contains diagonal and off-diagonal terms. A harmonic force of known amplitude and frequency is used to dynamically excite the beam. The present identification algorithms have been illustrated through numerical examples.

Ruotolo et al.[6] has investigated forced response of a cantilever beam with a crack that fully opens or closes, to determine depth and location of the crack. In their study, left end of the beam is cantilevered and right end is free. The harmonic sine force was applied on the free end of the beam. Vibration amplitude of the free end of the beam was taken into consideration. It was shown that vibration amplitude changes, when depth and location of the crack change.

Patil and Maiti [7,8] have utilized a method for prediction of location and size of multiple cracks based on measurement of natural frequencies has been verified experimentally for slender cantilever beams with two and three normal edge cracks. The analysis is based on energy method and representation of a crack by a rotational spring. For theoretical prediction the beam is divided into a number of segments and each segment is considered to be associated with a damage index. The damage index is an indicator of the extent of strain energy stored in the rotational spring. The crack size is computed using a standard relation between stiffness and crack size. Number of measured frequencies equal to twice the number of cracks is adequate for the prediction of location and size of all the cracks.

Kisa et al.[9,10] Presents a novel numerical technique applicable to analyse the free vibration analysis of uniform and stepped cracked beams with circular cross section. In this approach in which the finite element and component mode synthesis methods are used together, the beam is detached into parts from the crack section. These substructures are joined by using the flexibility matrices taking into account the interaction forces derived by virtue of fracture mechanics theory as the inverse of the compliance matrix found with the appropriate stress intensity factors and strain energy release rate expressions. To reveal the accuracy and effectiveness of the offered method, a number of numerical examples are given for free vibration analysis of beams with transverse non-propagating open cracks. Numerical results showing good agreement with the results of other available studies, address the effects of the location and depth of the cracks on the natural frequencies and mode shapes of the cracked beams. Modal characteristics of a cracked beam can be employed in the crack recognition process.

Loutridis et al.[11] present a new method for crack detection in beams based on instantaneous frequency and empirical mode decomposition is proposed. The dynamic behaviour of a cantilever beam with a breathing crack under harmonic excitation is investigated both theoretically and experimentally.

Darpe et al.[12] have studied Sa simple Jeffcott rotor with two transverse surface cracks. The stiffness of such a rotor is derived based on the concepts of fracture mechanics. Subsequently, the effect of the interaction of the two cracks on the breathing behavior and on the unbalance response of the rotor is studied.

Ertuğrul et al.[13] have studied to obtain information about the location and depth of cracks in cracked beams. For this purpose, the vibrations as a result of impact shocks were analyzed. The signals obtained in defect-free and cracked beams were compared in the frequency domain. The results of the study suggest to determine the location and depth of cracks by analyzing the from vibration signals. Experimental results and simulations obtained by the software ANSYS are in good agreement.

Fang et al.[14] have research, explore the structural damage detection using frequency response functions (FRFs) as input data to the back-propagation neural network (BPNN). Such method is non-model based and thus could have advantage in many practical applications. Neural network based damage detection generally consists of a training phase and a recognition phase. Error back-propagation algorithm incorporating gradient method can be applied to train the neural network, whereas the training efficiency heavily depends on the learning rate.

Suh et al. [15] has been established that a crack has an important effect on the dynamic behavior of a structure. This effect depends mainly on the location and depth of the crack. To identify the location and depth of a crack on a structure, a method is presented in this paper which uses hybrid neuro-genetic technique. Feed-forward multi-layer neural networks trained by back-propagation are used to learn the input and output relation of the structural system. With this trained neural network, genetic algorithm is used to identify the crack location and depth minimizing the difference from the measured frequencies.

Chondros et al. [16] has analyzed the lateral vibration of cracked Euler-Bernoulli beams with single or double edge cracks. Their analysis can be used for the prediction of the dynamic response of a simply supported beam with open surface cracks.

Rizos, et al. [17] has determined the crack location and its depth in a cantilever beam from the vibration modes. They achieved this by measuring the flexural vibrations of a cantilever beam with rectangular cross-section with a transverse surface crack. Analytical results are used to relate the measured vibration modes to the crack location and depth. From the measured amplitudes at two points of the structure vibrating at one of its natural modes, the respective vibration frequency and an analytical solution of the dynamic response, the crack location can be found and depth can be estimated with satisfactory accuracy.

Baris Binici [18] has proposed a new method is to obtain the Eigen frequencies and mode shapes of beams containing multiple cracks and subjected to axial force. Cracks are assumed to introduce local flexibility changes and are modeled as rotational springs. The method uses one set of end conditions as initial parameters for determining the mode shape functions. Satisfying

the continuity and jump conditions at crack locations, mode shape functions of the remaining parts are determined. Other set of boundary conditions yields a second-order determinant that needs to be solved for its roots. As the static case is approached, the roots of the characteristic equation give the buckling load of the structure.

Sekhar [19,20] applied the theory of model based identification in a rotor system with two cracks. In this work the crack induced change of the rotor system is taken into account by equivalent loads in the mathematical model. They have analysed the detection and monitoring of slant crack in the rotor system using mechanical impedance. The paper also synthesizes several works of the authors on cracked rotors to compare the two types of shaft cracks while studying flexural vibration characteristics. Eigenvalue analysis; steady state and transient response; crack detection based on changes in mechanical impedance and wavelet techniques have been discussed in order to compare slant crack with transverse crack.

Suresh et al.[21] have studied the flexural vibration in a cantilever beam having a transverse surface crack is considered. The modal frequency parameters are analytically computed for various crack locations and depths using a fracture mechanics based crack model. These computed modal frequencies are used to train a neural network to identify both the crack location and depth. The sensitivity of the modal frequencies to a crack increases when the crack is near the root and decreases as the crack moves to the free end of the cantilever beam. Because of the sensitive nature of this problem, a modular neural network approach is used.

Tsai and Wang [22] have investigated diagnostic method of determining the position and size of a transverse open crack on a stationary shaft without disengaging it from the machine system. The crack is modelled as a joint of a local spring. To obtain the dynamic characteristics of a stepped shaft and a multidisc shaft the transfer matrix method is employed on the basis of Timoshenko beam theory.

Zheng and Kessissoglou [23] have studied the natural frequencies and mode shapes of a cracked beam are obtained using the finite element method. An overall additional flexibility matrix, instead of the local additional flexibility matrix is added to the flexibility matrix of the

corresponding intact beam element to obtain the total flexibility matrix, and therefore the stiffness matrix. Compared with analytical results, the new stiffness matrix obtained using the overall additional flexibility matrix can give more accurate natural frequencies than those resulted from using the local additional flexibility matrix.

Hwang and Kim [24] have presents methods to identify the locations and severity of damage in structures using frequency response function data. Basic methods detect the location and severity of structural damage by minimizing the difference between test and analytic FRFs, which is a type of model updating or optimization method.

Fernandez-saez et al. [25] have presents simplified method of evaluating the fundamental frequency for the bending vibrations of cracked Euler–Bernouilli beams. The method is based on the well-known approach of representing the crack in a beam through a hinge and an elastic spring, but here the transverse deflection of the cracked beam is constructed by adding polynomial functions to that of the uncracked beam. With this new admissible function, which satisfies the boundary and the kinematic conditions, and by using the Rayleigh method, the fundamental frequency is obtained. This approach is applied to simply supported beams with a cracked section in any location of the span.

Chandra Kishen, et al. [26] have studied the fracture behavior of cracked beams and columns using finite element analysis. Assuming that failure occurs due to crack propagation when the mode I stress intensity factor reaches the fracture toughness of the material, the failure load of cracked columns are determined for different crack depths and slenderness ratios.

Sahin M. et al.[27] presents a damage detection algorithm using a combination of global (changes in natural frequencies) and local (curvature mode shapes) vibration-based analysis data as input in artificial neural networks (ANNs) for location and severity prediction of damage in beam-like structures. A finite element analysis tool has been used to obtain the dynamic characteristics of intact and damaged cantilever steel beams for the first three natural modes. Different damage scenarios have been introduced by reducing the local thickness of the selected elements at different locations along finite element model (FEM) of the beam structure.

Douka E.et al.[28] have investigated the influence of two transverse open cracks on the antiresonances of a double cracked cantilever beam both analytically and experimentally. It is shown that there is a shift in the antiresonances of the cracked beam depending on the location and size of the cracks. These antiresonance changes, complementary with natural frequency changes, can be used as additional information carrier for crack identification in double cracked beams.

Yoona Han-Ik et al.[29] have investigated the influence of two open cracks on the dynamic behavior of a double cracked simply supported beam both analytically and experimentally. The equation of motion is derived by using the Hamilton's principle and analyzed by numerical method. The simply supported beam is modeled by the Euler-Bernoulli beam theory.

Papadopoulos et al.[30] have used a method is applied in rotating cracked shafts to identify the depth and the location of a transverse surface crack. A local compliance matrix of different degrees of freedom is used to model the transverse crack in a shaft of circular cross section, based on available expressions of the stress intensity factors and the associated expressions for the strain energy release rates.

Behera [31] in his research work has developed the theoretical expressions to find out the natural frequencies and mode shapes for the cantilever beam with two transverse cracks. Experiments have been conducted to prove the authenticity of the theory developed

CHAPTER 3

CRACK THEORY

3. CRACK THEORY

3.1 Physical parameters affecting Dynamic characteristics of cracked structures:

Usually the physical dimensions, boundary conditions, the material properties of the structure play important role for the determination of its dynamic response. Their vibrations cause changes in dynamic characteristics of structures. In addition to this presence of a crack in structures modifies its dynamic behavior. The following aspects of the crack greatly influence the dynamic response of the structure.

(i) The position of crack

(ii) The depth of crack

(iii) The orientation of crack

(iv) The number of cracks

3.2 Classification of cracks

Based on their geometries, cracks can be broadly classified as follows:

- Cracks perpendicular to the beam axis are known as “transverse cracks”. These are the most common and most serious as they reduce the cross-section and thereby weaken the beam. They introduce a local flexibility in the stiffness of the beam due to strain energy concentration in the vicinity of the crack tip.
- Cracks parallel to the beam axis are known as “longitudinal cracks”. They are not that common but they pose danger when the tensile load is applied is at right angles to the crack direction i.e. perpendicular to beam axis or the perpendicular to crack.
- “Slant cracks” (cracks at an angle to the beam axis) are also encountered, but are not very common. These influence the torsion behavior of the beam. Their effect on lateral vibrations is less than that of transverse cracks of comparable severity.
- Cracks that open when the affected part of the material is subjected to tensile stresses and close when the stress is reversed are known as “breathing cracks”. The stiffness of the component is most influenced when under tension. The breathing of the crack results in non-linearity’s in the vibration behavior of the beam. Cracks breathe when crack sizes are small, running speeds are low and radial forces are large .Most

theoretical research efforts are concentrated on “transverse breathing” cracks due to their direct practical relevance.

- Cracks that always remain open are known as “gaping cracks”. They are more correctly called “notches”. Gaping cracks are easy to mimic in a laboratory environment and hence most experimental work is focused on this particular crack type.
- Cracks that open on the surface are called “surface cracks”. They can normally be detected by techniques such as dye-penetrates or visual inspection.
- Cracks that do not show on the surface are called “subsurface cracks”. Special techniques such as ultrasonic, magnetic particle, radiography or shaft voltage drop are needed to detect them. Surface cracks have a greater effect than subsurface cracks on the vibration behavior of shafts.

3.3 Modes of Fracture: -The three basic types of loading that a crack experiences are

- **Mode I** corresponds to the opening mode in which the crack faces separates in a direction normal to the plane of the crack and the corresponding displacements of crack walls are symmetric with respect to the crack front. Loading is normal to the crack plane, and tends to open the crack. Mode I is generally considered the most dangerous loading situation.
- **Mode II** corresponds to in-plane shear loading and tends to slide one crack face with respect to the other (shearing mode). The stress is parallel to the crack growth direction.
- **Mode III** corresponds to out-of-plane shear, or tearing. In which the crack faces are sheared parallel to the crack front.

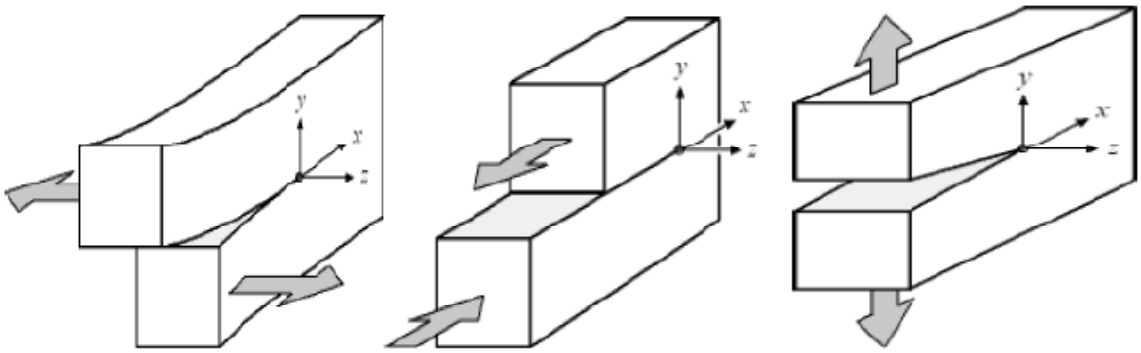

Fig.3.1. Three basic mode of fracture.

3.4 Stress Intensity Factor (SIF), K: - It is defined as a measure of the stress field intensity near the tip of an ideal crack in a linear elastic solid when the crack surfaces are displaced in the opening mode (Mode I). (SIFs) are used to define the magnitude of the singular stress and displacement fields (local stresses and displacements near the crack tip). The SIF depends on the loading, the crack size, the crack shape, and the geometric boundaries of the specimen. The recommended units for K are MPa√m. it is customary to write the general formula in the form $K=Y\sigma\sqrt{\pi a}$ where σ is the applied stress, a is crack depth, Y is dimensionless shape factor.

CHAPTER 4

THEORITICAL ANALYSIS

4. THEORITICAL ANALYSIS

The beam with a two transverse edge cracks is clamped at left end, free at right end and it has a uniform structure with a constant rectangular cross-section. The Euler–Bernoulli beam model was assumed. The damping has not been considered in this study. A cantilever beam of length L, of uniform rectangular cross-section $B \times W$ with cracks located at positions L_1 and L_2 is considered in fig.(4.1). The cracks are assumed to be an open crack and have uniform depths a_1 and a_2 respectively. In the present analysis the axial and bending vibration are considered.

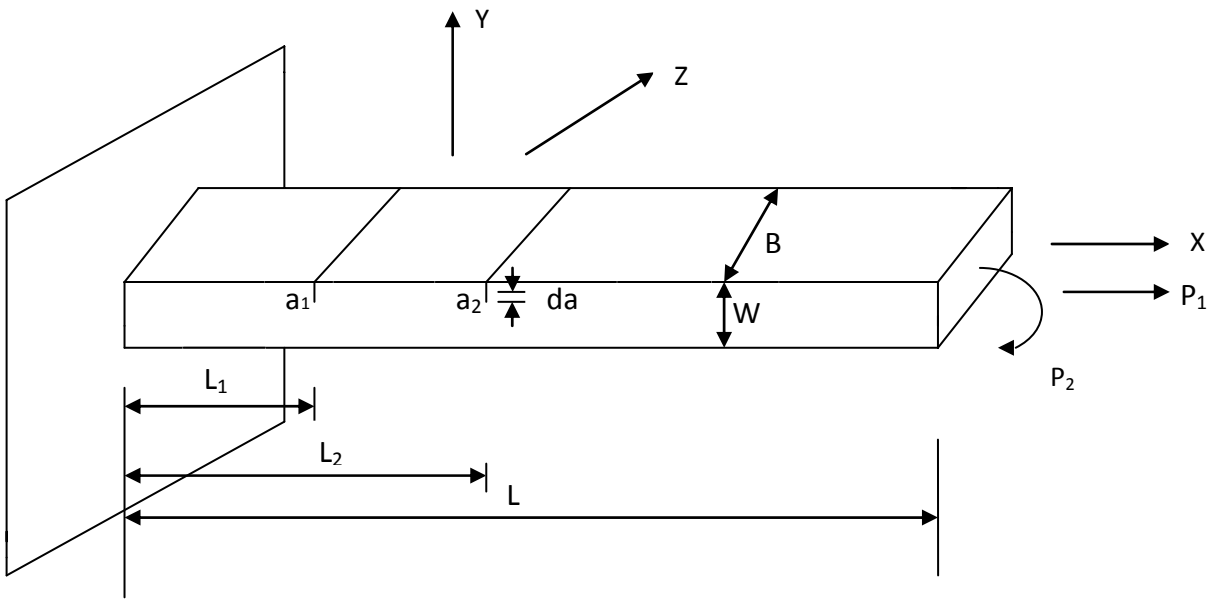

Fig.4.1. Geometry of cantilever beam with two transverse cracks.

Local flexibility of cracked beam under bending and axial loading

The present of crack of depth a_1 introduces a local flexibility matrix. The dimension of the local flexibility matrix (2×2), as each side has two degree of freedom where off diagonal elements of the matrix are considered as coupling elements in the flexibility matrix. The elastic strain energy release rate J can be expressed as follows,

$$J(a)=\frac{1}{E'}(KI_1+KI_2)^2 \qquad (4.1)$$

Where $E^{'}=E/1-\upsilon^2$ for plain strain.

The stress intensity factors from elementary fracture mechanics are given as

$$KI_1=\frac{P_1}{BW}\sqrt{\pi a}\{F_1(a/W)\} \qquad (4.2)$$

$$KI_2=\frac{6P_2}{BW^2}\sqrt{\pi a}\{F_2(a/W)\} \qquad (4.3)$$

Where B and W are the cross-section dimensions and a is crack depth as shown in fig.4.2.

KI_1 and KI_2 are the stress intensity factors of Mode I(opening of the crack) for axial force P_1 and bending moment P_2 respectively. To guarantee the open crack mode the beam is assumed to be preloaded by its own weight. The amplitude of vibration is assumed to be well below the crack opening due to preloading.

The function F_1 and F_2 are dependent on the crack depth and approximated as [32]

$$F_1\left(\frac{a}{W}\right)=\left(\frac{2W}{\pi a}\tan(\pi a/2W)\right)^{0.5}\left\{\frac{0.752+2.02(a/W)+0.37\left(1-\sin(\pi a/2W)\right)^3}{\cos(\pi a/2W)}\right\}$$

$$F_2\left(\frac{a}{W}\right)=\left(\frac{2W}{\pi a}\tan(\pi a/2W)\right)^{0.5}\left\{\frac{0.923+0.199(1-\sin(\pi a/2W))^4}{\cos(\pi a/2W)}\right\}$$

In addition crack produces a local additional displacement u_i between the right and left sections of the crack, in similar way as equivalent spring. These displacement u_i in the i direction under the action of force P_i are be given as castiliagno's theorem [33].

$$u_i=\frac{\partial}{\partial P_i}\left[\int_0^{a_1} J(a)da\right] \qquad (4.4)$$

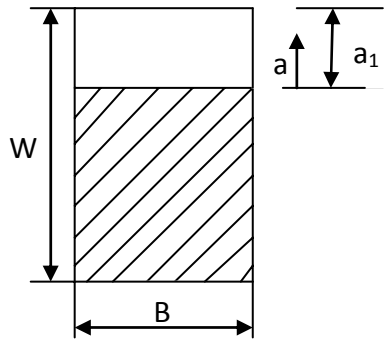

Fig.4.2.Geometry of cracked section of cantilever beam

Finally the additional flexibility introduced due to crack is obtained by combining relation (4.3) and (4.4) and definition of compliance [33].

$$C_{ij}=\frac{\partial u_i}{\partial P_j}=\frac{\partial^2}{\partial P_i \partial P_j}\int_0^{a_1} J(a)da \qquad (4.5)$$

The final flexibility matrix can be formed by integrating over the breadth B of beam.

$$C_{ij}=\frac{\partial u_i}{\partial P_j}=\frac{\partial^2}{\partial P_i \partial P_j}\int_{-B/2}^{+B/2}\int_0^{a_1} J(a)dadz \qquad (4.6)$$

Putting the value of strain energy release rate equation (4.6) can be modified,

$$C_{ij}=\frac{B}{E'}\frac{\partial^2}{\partial P_i \partial P_j}\int_0^{a_1}(KI_1+KI_2)^2 da \qquad (4.7)$$

Writing $\xi = a/W$ are obtains $d\xi = da/W$

We get $da = Wd\xi$ and When $a=0$, $\xi=0$ and When $a = a_1$, $\xi = a_1/W = \xi_1$

From above condition equation (4.7) becomes

$$C_{ij}=\frac{BW}{E'}\frac{\partial^2}{\partial P_i \partial P_j}\int_0^{\xi_1}(KI_1+KI_2)^2 d\xi \qquad (4.8)$$

From equation (4.8) local axial, coupled axial and bending and bending compliance can be calculated as

$$C_{11}=\frac{BW}{E'}\int_0^{\xi_1}\frac{\pi a}{B^2W^2}2\left(F_1(\xi)\right)^2 d\xi$$

$$C_{11}=\frac{2\pi}{BE'}\int_0^{\xi_1}\xi\left(F_1(\xi)\right)^2 d\xi \qquad (4.9)$$

$$C_{12}=C_{21}=\frac{12\pi}{BWE'}\int_0^{\xi_1}\xi\, F_1(\xi)F_2(\xi)d\xi \qquad (4.10)$$

$$C_{22}=\frac{72\pi}{E'BW^2}\int_0^{\xi_1}\xi\, F_2(\xi)F_2(\xi)d\xi \qquad (4.11)$$

In dimensionless form the above equation (4.9) to (4.11) can be written as

$$\bar{C}_{11}=C_{11}\frac{BE'}{2\pi} \qquad (4.12)$$

$$\bar{C}_{12}=C_{12}\frac{E'BW}{12\pi}=\bar{C}_{21} \qquad (4.13)$$

$$\bar{C}_{22} = C_{22}\frac{E'BW^2}{72\pi} \qquad (4.14)$$

The local stiffness matrix can be obtained by taking inverse of compliance matrix.

$$K=\begin{bmatrix} k_{11} & k_{12} \\ k_{21} & k_{22} \end{bmatrix}=\begin{bmatrix} c_{11} & c_{12} \\ c_{21} & c_{22} \end{bmatrix}^{-1}$$

The stiffness matrix of first crack

$$K'=\begin{bmatrix} c'_{11} & c'_{12} \\ c'_{21} & c'_{22} \end{bmatrix}^{-1}$$

The stiffness matrix of Second crack

$$K''=\begin{bmatrix} c''_{22} & c''_{23} \\ c''_{32} & c''_{33} \end{bmatrix}^{-1}$$

4.1. Governing equation of free vibration

Fig.4.3 shows a double-cracked cantilever beam with longitudinal and transverse vibrations. Here, $U_1(x,t)$, $U_2(x,t)$ and $U_3(x,t)$ are longitudinal vibrations for the section before and after the cracks. Moreover, $Y_1(x,t)$, $Y_2(x,t)$ and $Y_3(x,t)$ are bending vibrations for the same section(fig.4.3).

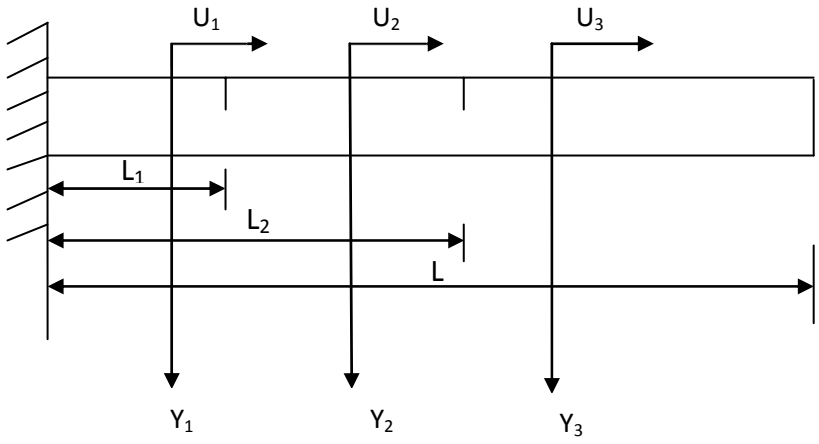

Fig.4.3. Beam Model with cracks.

The normal functions for the system can be defined as

$$\bar{u}_1(\bar{x})=A_1\cos(\bar{k}_u\bar{x})+A_2\sin(\bar{k}_u\bar{x}) \qquad (4.15)$$

$\bar{u}_2(\bar{x})=A_3\cos(\bar{k}_u\bar{x})+A_4\sin(\bar{k}_u\bar{x})$ (4.16)

$\bar{u}_3(\bar{x})=A_5\cos(\bar{k}_u\bar{x})+A_6\sin(\bar{k}_u\bar{x})$ (4.17)

$\bar{y}_1(\bar{x})=A_7\cosh(\bar{k}_y\bar{x})+A_8\sinh(\bar{k}_y\bar{x})+A_9\cos(\bar{k}_y\bar{x})+A_{10}\sin(\bar{k}_y\bar{x})$ (4.18)

$\bar{y}_2(\bar{x})=A_{11}\cosh(\bar{k}_y\bar{x})+A_{12}\sinh(\bar{k}_y\bar{x})+A_{13}\cos(\bar{k}_y\bar{x})+A_{14}\sin(\bar{k}_y\bar{x})$ (4.19)

$\bar{y}_3(\bar{x})=A_{15}\cosh(\bar{k}_y\bar{x})+A_{16}\sinh(\bar{k}_y\bar{x})+A_{17}\cos(\bar{k}_y\bar{x})+A_{18}\sin(\bar{k}_y\bar{x})$ (4.20)

where

$\bar{x}=x/L$, $\bar{u}=u/L$, $\bar{y}=y/L$, $\bar{t}=t/T$, $\beta=L_1/L$, $\gamma=L_2/L$

$\bar{k}_u=\omega L/C_u$, $C_u=\left(E/\rho\right)^{1/2}$, $\bar{k}_y=(\omega L^2/C_y)^{1/2}$, $C_y=(EI/\mu)^{1/2}$, $\mu=A\rho$

$A_{i,}(i=1,18)$ are the constants to be determined by the boundary conditions.

The associated boundary conditions for the cracked cantilever beam under consideration are:

$\bar{u}_1(0)=0$ (4.21)

$\bar{y}_1(0)=0$ (4.22)

$\bar{y}_1'(0)=0$ (4.23)

$\bar{u}_3'(1)=0$ (4.24)

$\bar{y}_3''(1)=0$ (4.25)

$\bar{y}_3'''(1)=0$ (4.26)

At the cracked section, we have:

$\bar{u}_1'(\beta)=\bar{u}_2'(\beta)$ (4.27)

$\bar{y}_1(\beta)=\bar{y}_2(\beta)$ (4.28)

$\bar{y}_1''(\beta)=\bar{y}_2''(\beta)$ (4.29)

$\bar{y}_1'''(\beta)=\bar{y}_2'''(\beta)$ (4.30)

$\bar{u}_2'(\gamma)=\bar{u}_3'(\gamma)$ (4.31)

$\bar{y}_2(\gamma)=\bar{y}_3(\gamma)$ (4.32)

$\bar{y}_2''(\gamma)=\bar{y}_3''(\gamma)$ (4.33)

$\bar{y}_2'''(\gamma)=\bar{y}_3'''(\gamma)$ (4.34)

Also at the cracked section, we have:

$$AE\frac{du_1(L_1)}{dx}=k'_{11}(u_2(L_1)-u_1(L_1))+k'_{12}\left(\frac{dy_2(L_1)}{dx}-\frac{dy_1(L_1)}{dx}\right)$$

Multiplying both sides by $AE/Lk'_{11}k'_{12}$ and simplifying we get

$$m_1 m_2 \bar{u}'_1(\beta) = m_2(\bar{u}_2(\beta)-\bar{u}'_1(\beta))+m_1(\bar{y}'_2(\beta)-\bar{y}'_1(\beta)) \quad (4.35)$$

Similarly,

$$EI\frac{d^2y_1(L_1)}{dx^2} = k'_{21}(u_2(L_1)-u_1(L_1))+k'_{22}\left(\frac{dy_2(L_1)}{dx}-\frac{dy_1(L_1)}{dx}\right)$$

Multiplying both sides $EI/L^2k'_{22}k'_{21}$ and simplifying we get,

$$m_3 m_4 \bar{y}''_1(\beta) = m_4(\bar{y}'_2(\beta)-\bar{y}'_1(\beta))+ m_3(\bar{u}_2(\beta)-\bar{u}_1(\beta)) \quad (4.36)$$

Similarly for the position of second crack from the fixed end we have

$$m_5 m_6 \bar{u}'_2(\gamma) = m_6(\bar{u}_3(\gamma)-\bar{u}_2(\gamma))+ m_5(\bar{y}'_3(\gamma)-\bar{y}'_2(\gamma)) \quad (4.37)$$

$$m_7 m_8 \bar{y}''_2(\gamma) = m_8(\bar{y}'_3(\gamma)-\bar{y}'_2(\gamma))+ m_7(\bar{u}_3(\gamma)-\bar{u}_2(\gamma)) \quad (4.38)$$

Where $m_1=AE/(Lk'_{11})$, $m_2=AE/k'_{12}$, $m_3=EI/(Lk'_{22})$, $m_4=EI/(L^2k'_{21})$

$m_5=AE/(Lk'_{22})$, $m_6=AE/k''_{23}$, $m_7=EI/(Lk''_{33})$, $m_8=EI/(L^2k''_{32})$

The natural frequency of the cracked beam can be evaluated using the crack model and boundary conditions. The stiffness matrices and equation (4.21)-(4.38) define these relations as set of 18 homogeneous linear equations. These equations can be written in compact form as

$$[Q]\{A\}= \{0\} \quad (4.39)$$

Where [Q] is the coefficient matrix defined in terms of the cracked beam parameters & given as:

$$[Q]=\begin{bmatrix}
0 & 0 & 0 & 0 & 0 & 0 & 0 & 0 & 0 & 0 & 0 & 1 & 0 & 0 & 0 & 0 & 0 & 0 \\
1 & 0 & 0 & 0 & 0 & 0 & 0 & 0 & 0 & 0 & 0 & 0 & 0 & 0 & 0 & 0 & 0 & 0 \\
0 & 1 & 0 & 1 & 0 & 0 & 0 & 0 & 0 & 0 & 0 & 0 & 0 & 0 & 0 & 0 & 0 & 0 \\
0 & 0 & 0 & 0 & 0 & 0 & 0 & 0 & 0 & 0 & 0 & 0 & 0 & 0 & 0 & 0 & -T_1 & T_2 \\
0 & 0 & 0 & 0 & 0 & 0 & 0 & 0 & G_3 & G_4 & -G_7 & -G_8 & 0 & 0 & 0 & 0 & 0 & 0 \\
0 & 0 & 0 & 0 & 0 & 0 & 0 & 0 & G_4 & G_3 & G_8 & -G_7 & 0 & 0 & 0 & 0 & 0 & 0 \\
0 & 0 & 0 & 0 & 0 & 0 & 0 & 0 & 0 & 0 & 0 & 0 & -T_6 & T_5 & T_6 & -T_5 & 0 & 0 \\
G_1 & G_2 & G_5 & G_6 & -G_1 & -G_2 & -G_5 & -G_6 & 0 & 0 & 0 & 0 & 0 & 0 & 0 & 0 & 0 & 0 \\
G_1 & G_2 & -G_5 & -G_6 & -G_1 & -G_2 & G_5 & G_6 & 0 & 0 & 0 & 0 & 0 & 0 & 0 & 0 & 0 & 0 \\
G_2 & G_1 & G_6 & -G_5 & -G_2 & -G_1 & -G_6 & G_5 & 0 & 0 & 0 & 0 & 0 & 0 & 0 & 0 & 0 & 0 \\
0 & 0 & 0 & 0 & 0 & 0 & 0 & 0 & 0 & 0 & 0 & 0 & 0 & 0 & -T_4 & T_3 & T_4 & -T_3 \\
0 & 0 & 0 & 0 & G_9 & G_{10} & G_{11} & G_{12} & -G_9 & -G_{10} & -G_{11} & -G_{12} & 0 & 0 & 0 & 0 & 0 & 0 \\
0 & 0 & 0 & 0 & G_9 & G_{10} & -G_{11} & -G_{12} & -G_9 & -G_{10} & G_{11} & G_{12} & 0 & 0 & 0 & 0 & 0 & 0 \\
0 & 0 & 0 & 0 & G_{10} & G_9 & G_{12} & -G_{11} & -G_{10} & -G_9 & -G_{12} & G_{11} & 0 & 0 & 0 & 0 & 0 & 0 \\
-S_3 & -S_4 & S_5 & -S_6 & S_3 & S_4 & -S_5 & S_6 & 0 & 0 & 0 & 0 & S_1 & -S_2 & T_5 & T_6 & 0 & 0 \\
S_7 & S_8 & -S_9 & -S_{10} & -S_{11} & -S_{12} & S_{13} & -S_{14} & 0 & 0 & 0 & 0 & S_{15} & S_{16} & -S_{15} & -S_{16} & 0 & 0 \\
0 & 0 & 0 & 0 & V_3 & V_4 & -V_5 & V_6 & -V_3 & -V_4 & V_5 & -V_6 & 0 & 0 & V_1 & V_2 & -T_3 & -T_4 \\
0 & 0 & 0 & 0 & V_7 & V_8 & -V_9 & -V_{10} & -V_{11} & -V_{12} & V_{13} & -V_{14} & 0 & 0 & V_{15} & V_{16} & -V_{15} & -V_{16}
\end{bmatrix}$$

Where, $T_1=\sin\bar{k}_u$, $T_2=\cos\bar{k}_u$, $T_3=\cos(\bar{k}_u\gamma)$, $T_4=\sin(\bar{k}_u\gamma)$, $T_5=\cos(\bar{k}_u\beta)$, $T_6=\sin(\bar{k}_u\beta)$,

$G_1=\cosh(\bar{k}_y\beta)$, $G_2=\sinh(\bar{k}_y\beta)$, $G_3=\cosh(\bar{k}_y)$, $G_4=\sinh(\bar{k}_y)$ $G_5=\cos(\bar{k}_y\beta)$, $G_6=\sin(\bar{k}_y\beta)$,

$G_7=\cos(\bar{k}_y)$, $G_8=\sin(\bar{k}_y)$, $G_9=\cosh(\bar{k}_y\gamma)$, $G_{10}=\sinh(\bar{k}_y\gamma)$, $G_{11}=\cos(\bar{k}_y\gamma)$, $G_{12}=\sin(\bar{k}_y\gamma)$,

$m_1=AE/(Lk'_{11})$, $m_2=AE/k'_{12}$, $m_3=EI/(Lk'_{22})$, $m_4=EI/(L^2k'_{21})$, $m_{12}=m_1/m_2$, $m_{34}=m_3/m_4$,

$S_1=T_5-m_1\bar{k}_uT_6$, $S_2=T_6+m_1\bar{k}_uT_5$, $S_3=m_{12}S_{11}$, $S_3=m_{12}S_{12}$, $S_5=m_{12}S_{13}$, $S_6=m_{12}S_{14}$

$S_7=m_3\bar{k}_y^2G_1+S_{11}$, $S_8=m_3\bar{k}_y^2G_2+S_{12}$, $S_9=m_3\bar{k}_y^2G_5+S_{13}$, $S_{10}=m_3\bar{k}_y^2G_6-S_{14}$,

$S_{11}=\bar{k}_yG_2$, $S_{12}=\bar{k}_yG_1$, $S_{13}=\bar{k}_yG_6$, $S_{14}=\bar{k}_yG_5$, $S_{15}=m_{34}T_5$, $S_{16}=m_{34}T_6$

$m_5=AE/(Lk''_{22})$, $m_6=AE/k''_{23}$, $m_7=EI/(Lk''_{33})$, $m_8=EI/(Lk''_{32})$, $m_{56}=m_5/m_6$,

$m_{78}=m_7/m_8$, $V_1=T_3-m_5\bar{k}_uT_4$, $V_2=T_4+m_5\bar{k}_uT_3$, $V_3=m_{56}V_{11}$, $V_4=m_{56}V_{12}$,

$V_5=m_{56}V_{13}$, $V_6=m_{56}V_{14}$, $V_7=m_7\bar{k}_y^2G_9+V_{11}$, $V_8=m_7\bar{k}_y^2G_{10}+V_{12}$,

$V_9=m_7\bar{k}_y^2G_{11}+V_{13}$, $V_{10}=m_7\bar{k}_y^2G_{12}-V_{14}$, $V_{11}=\bar{k}_yG_{10}$, $V_{12}=\bar{k}_yG_9$, $V_{13}=\bar{k}_yG_{12}$,

$V_{14}=\bar{k}_yG_{11}$, $V_{15}=m_{78}T_3$, $V_{16}=m_{78}T_4$

The vector $\{A\}= [A_1,...,A_{18}]^T$ contains the coefficients used in equations (4.15-4.20). For non trivial values for the vector {A}, equation (4.39) leads to the following characteristic equation:

$|Q|=0$ .....(21)

Given all the cracked beam parameters, the only unknown in equation (4.40) is the value of the natural frequency ω. The root of the characteristic equation $|Q|$ gives the values of natural frequencies. The frequency of identical uncracked beam is obtained by modifying equation (4.40), where crack relations are removed and only equations describing the boundary conditions are applied resulting in a 6×6 characteristic matrix. The mode shapes for the transverse & axial vibration are determined by evaluating the vector $\{A\}= [A_1,...,A_{18}]^T$. This done by setting the value of A_5 to 1,then solving for the rest of the elements using equation (4.39) after the required modifications.

4.2. Governing equations of forced vibration

If the cantilever beam with transverse cracks is excited at its free end by harmonic excitation ($Y= Y_0 \sin\omega t$), the non dimensional amplitude at the free end may be expressed $\bar{y}_3(1) = y_0/L = \bar{y}_0$, therefore the boundary condition for beam remain the same as before except in the case of the case of expression equation(4.26), which is change to as $\bar{y}_3(1)=\bar{y}_0$.

The constants A_i (i=1,18) are computed from the algebraic condition $Q_1D=B_1$, where Q is (18×18) matrix obtained from the constants, & B_1 is a column matrix whose transpose is given by

$B_1^T=[0 \quad 0 \quad 0 \quad \bar{y}_0 \quad 0 \quad 0 \quad 0 \quad 0 \quad 0 \quad 0 \quad 0 \quad 0 \quad 0 \quad 0 \quad 0 \quad 0 \quad 0 \quad 0 \quad 0]$

CHAPTER 5

NEURAL NETWORK

5. NEURAL NETWORK

Studies on neural networks have been motivated to imitate the way that the brain operates. A network is described in terms of the individual neurons, the network connectivity, the weights associated with various interconnections between neurons, and the activation function for each neuron. The network maps an input vector from one space to another. The mapping is not specified, but is learned. The network is presented with a given set of inputs and their associated outputs. The learning process is used to determine proper interconnection weights and the network is trained to make proper associations between the inputs and their corresponding outputs. Once trained, the network provides rapid mapping of a given input into the desired output quantities. This, in turn, can be used to enhance the efficiency of the design process.

5.1 NEURON STRUCTURE

The perceptron is a single level connection of McCulloch-Pitts neurons sometimes called single-layer feed-forward networks. The network is capable of linearly separating the input vectors into pattern of classes by a hyper plane. A linear associative memory is an example of a single-layer neural network. In such an application, the network associates an output pattern (vector) with an input pattern (vector), and information is stored in the network by virtue of modifications made to the synaptic weights of the network.

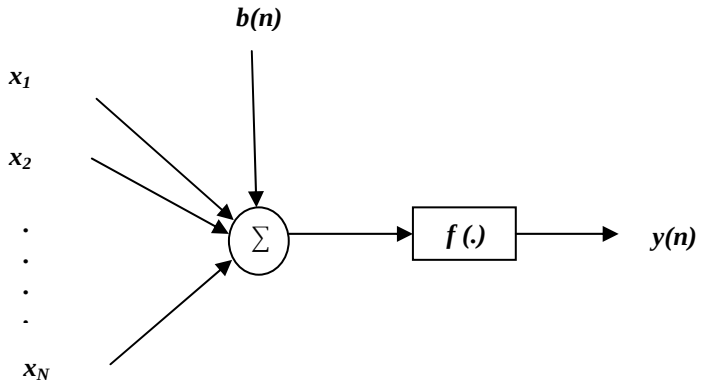

Fig 5.1 Neuron Structure

The structure of a single neuron is presented in Fig. 5.1. An artificial neuron involves the computation of the weighted sum of inputs and threshold [33]. The resultant signal is then

passed through a non-linear activation function. The output of the neuron may be represented as,

$$y(n) = f\left[\sum_{j=1}^{N} w_j(n)x_j(n) + b(n)\right] \quad (5.1)$$

where, $b(n)$ = threshold to the neuron is called as bias, $w_j(n)$ = weight associated with the j^{th} input, and N = no. of inputs to the neuron.

5.1.1. Activation Functions and Bias:

The perceptron internal sum of the inputs is passed through an activation function, which can be any monotonic function. Linear functions can be used but these will not contribute to a non-linear transformation within a layered structure, which defeats the purpose of using a neural filter implementation. A function that limits the amplitude range and limits the output strength of each perceptron of a layered network to a defined range in a non-linear manner will contribute to a nonlinear transformation. There are many forms of activation functions, which are selected according to the specific problem. All the neural network architectures employ the activation function [34] which defines as the output of a neuron in terms of the activity level at its input (ranges from -1 to 1 or 0 to 1). Table 5.1 summarizes the basic types of activation functions. The most practical activation functions are the sigmoid and the hyperbolic tangent functions. This is because they are differentiable.

The bias gives the network an extra variable and the networks with bias are more powerful than those of without bias. The neuron without a bias always gives a net input of zero to the activation function when the network inputs are zero. This may not be desirable and can be avoided by the use of a bias.

Table 5.1 Types of Activation Functions

NAME	**MATHEMATICAL REPRESENTATION**
Linear	$f(x) = kx$
Step	$f(x) = \begin{cases} \alpha, & if\ x \geq k \\ \beta, & if\ x < k \end{cases}$
Sigmoid	$f(x) = \frac{1}{1+e^{-\alpha x}}\ , \alpha > 0$
Hyperbolic Tangent	$f(x) = \frac{1-e^{-\gamma x}}{1+e^{-\gamma x}}, \gamma\ > 0$
Gaussian	$f(x) = \frac{1}{\sqrt{2\pi\sigma^2}} e^{\left[-\frac{(x-\mu)^2}{2\sigma^2}\right]}$

5.1.2 Learning Technique:

The property that is of primary significance for a neural network is that the ability of the network to learn from its environment, and to improve its performance through learning. The improvement in performance takes place over time in accordance with some prescribed measure. A neural network learns about its environment through an interactive process of adjustments applied to its synaptic weights and bias levels. Ideally, the network becomes more knowledgeable about its environment after each iteration of learning process. Hence we define learning as:

"It is a process by which the free parameters of a neural network are adapted through a process of stimulation by the environment in which the network is embedded."

The processes used are classified into two categories as described in:

(i) Supervised Learning (Learning With a Teacher)

(ii) Unsupervised Learning (Learning Without a Teacher)

(i) *Supervised Learning:*

We may think of the teacher as having knowledge of the environment, with that knowledge being represented by a set of input-output examples. The environment is, however unknown to neural network of interest. Suppose now the teacher and the neural network are both exposed to a training vector, by virtue of built-in knowledge, the teacher is able to provide the neural network with a desired response for that training vector. Hence the desired response represents the optimum action to be performed by the neural network. The network parameters such as the weights and the thresholds are chosen arbitrarily and are updated during the training procedure to minimize the difference between the desired and the estimated signal. This updation is carried out iteratively in a step-by-step procedure with the aim of eventually making the neural network emulate the teacher. In this way knowledge of the environment available to the teacher is transferred to the neural network. When this condition is reached, we may then dispense with the teacher and let the neural network deal with the environment completely by itself. This is the form of supervised learning.

By applying this type of learning technique, the weights of neural network are updated by using LMS algorithm. The update equations for weights are derived as LMS[33,34]:

$$w_j(n+1) = w_j(n) + \mu \Delta w_j(n) \tag{5.2}$$

(ii) *Unsupervised Learning:*

In unsupervised learning or self-supervised learning there is no teacher to over-see the learning process, rather provision is made for a task independent measure of the quantity of representation that the network is required to learn, and the free parameters of the network are optimized with respect to that measure. Once the network has become turned to the statistical regularities of the input data, it develops the ability to form the internal representations for encoding features of the input and thereby to create new classes automatically. In this learning the weights and biases are updated in response to network input only. There are no desired outputs available. Most of these algorithms perform some kind of clustering operation. They learn to categorize the input patterns into some classes.

5.2. MULTILAYER PERCEPTRON

In the multilayer neural network or multilayer perceptron (MLP), the input signal propagates through the network in a forward direction, on a layer-by-layer basis. This network has been applied successfully to solve some difficult and diverse problems by training in a supervised manner with a highly popular algorithm known as the error back-propagation algorithm [33]. The scheme of MLP using four layers is shown in Fig.5.2. $x_i(n)$ represents the input to the network, f_j and f_k represent the output of the two hidden layers and $y_i(n)$ represents the output of the final layer of the neural network. The connecting weights between the input to the first hidden layer, first to second hidden layer and the second hidden layer to the output layers are represented by respectively.

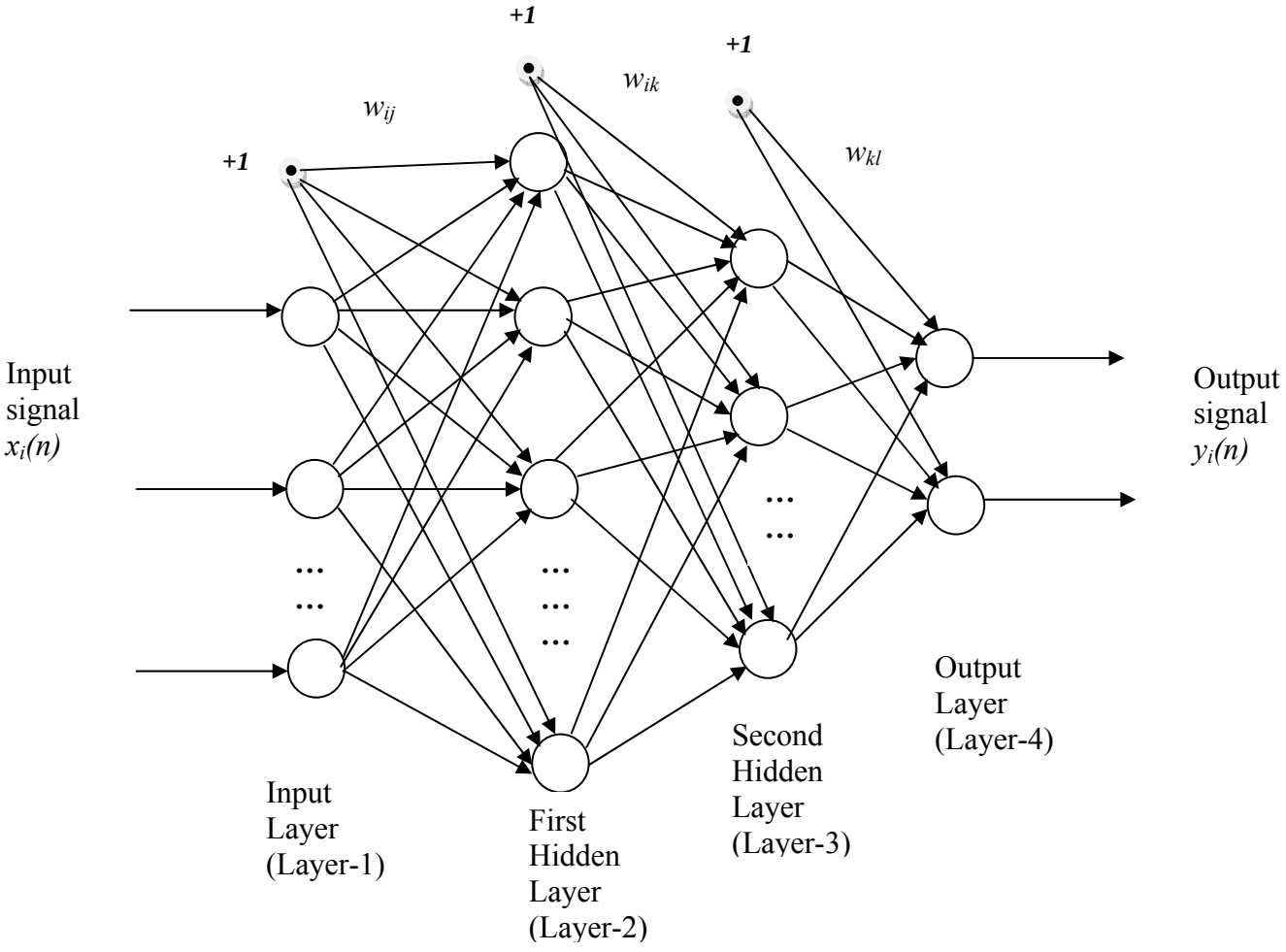

Fig 5.2 Structure of Multilayer Perceptron

If P_1 is the number of neurons in the first hidden layer, each element of the output vector of first hidden layer may be calculated as,

$$f_j = \varphi_j\left[\sum_{i=1}^{N} w_{ij}x_i(n) + b_j\right], i = 1,2,\ldots N, j = 1,2,\ldots P_1 \qquad (5.3)$$

where b_j is the threshold to the neurons of the first hidden layer, N is the no. of inputs and φ is the nonlinear activation function in the first hidden layer chosen from the Table 5.1. The time index n has been dropped to make the equations simpler. Let P_2 be the number of neurons in the second hidden layer. The output of this layer is represented as, f_k and may be written as

$$f_k = \varphi_k\left[\sum_{j=1}^{P_1} w_{jk}f_j + b_k\right], k = 1,2,\ldots . P_2 \qquad (5.4)$$

where, b_k is the threshold to the neurons of the second hidden layer. The output of the final output layer can be calculated as

$$y_l(n) = \varphi_l\left[\sum_{k=1}^{P_2} w_{kl}f_k + b_l\right], l = 1,2,\ldots P_3 \qquad (5.5)$$

where, b_l is the threshold to the neuron of the final layer and P_3 is the no. of neurons in the output layer. The output of the MLP may be expressed as

$$y_l(n) = \varphi_l\left[\sum_{k=1}^{P_2} w_{kl}\left(\varphi_k\left[\sum_{j=1}^{P_1} w_{jk}\left(\varphi_j\left[\sum_{i=1}^{N} w_{ij}x_i(n) + b_j\right]\right) + b_k\right]\right) + b_l\right] \qquad (5.6)$$

5.2.1 Back propagation Algorithm

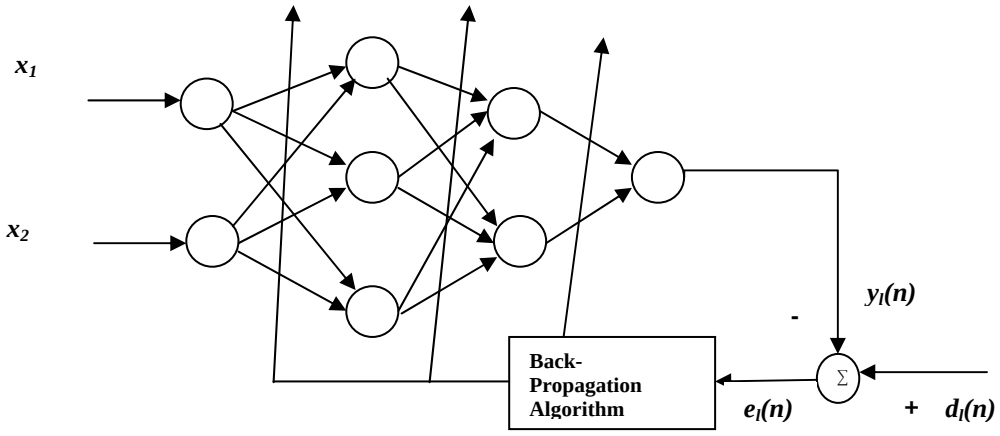

Fig 5.3 Neural Network with Back Propagation Algorithm

An MLP network with 2-3-2-1 neurons (2, 3, 2 and 1 denote the number of neurons in the input layer, the first hidden layer, the second hidden layer and the output layer respectively) with the back-propagation (BP) learning algorithm, is depicted in Fig.5.3. The parameters of the neural network can be updated in both sequential and batch mode of operation. In BP algorithm, initially the weights and the thresholds are initialized as very small random values. The intermediate and the final outputs of the MLP are calculated by using (5.3), (5.4), and (5.5) respectively.

The final output $y_l(n)$ at the output of neuron l, is compared with the desired output $d(n)$ and the resulting error signal $e(n)$ is obtained as

$$e_l(n) = d(n) - y_l(n) \tag{5.7}$$

The instantaneous value of the total error energy is obtained by summing all error signals over all neurons in the output layer, that is

$$\xi(n) = \frac{1}{2} \sum_{l=1}^{P_3} e_l^2(n) \tag{5.8}$$

where P_3 is the no. of neurons in the output layer.

This error signal is used to update the weights and thresholds of the hidden layers as well as the output layer. The reflected error components at each of the hidden layers is computed using the errors of the last layer and the connecting weights between the hidden and the last layer and error obtained at this stage is used to update the weights between the input and the hidden layer. The thresholds are also updated in a similar manner as that of the corresponding connecting weights. The weights and the thresholds are updated in an iterative method until the error signal become minimum. For measuring the degree of matching, squared error cannot be considered as the network may have multiple outputs and Root Mean Square Error (RMSE) cause over fitting of the model and the weights may not converge. So the Mean Square Error (MSE) is taken as a performance measurement.

The weights are using the following formulas,

$$w_{kl}(n+1) = w_{kl}(n) + \Delta w_{kl}(n) \tag{5.9}$$

$$w_{jk}(n+1) = w_{jk}(n) + \Delta w_{jk}(n) \quad (5.10)$$

$$w_{ij}(n+1) = w_{ij}(n) + \Delta w_{ij}(n) \quad (5.11)$$

$$\Delta w_{kl}(n) = -2\mu \frac{\partial \xi(n)}{\partial w_{kl}(n)} = \mu e(n) \frac{dy_l(n)}{dw_{kl}(n)}$$

$$= \mu e(n) \varphi_l' \left[\sum_{k=1}^{P_2} w_{kl} f_k + b_l\right] f_k \quad (5.12)$$

Where, μ is the convergence coefficient (0<μ<1). Similarly $\Delta w_{jk}(n)$ and $\Delta w_{ij}(n)$ the can be computed.

The thresholds of each layer can be updated in a similar manner, i.e.

$$b_l(n+1) = b_l(n) + \Delta b_l(n) \quad (5.13)$$

$$b_k(n+1) = b_k(n) + \Delta b_k(n) \quad (5.14)$$

$$b_j(n+1) = b_j(n) + \Delta b_j(n) \quad (5.15)$$

where, $\Delta b_l(n)$, $\Delta b_k(n)$ and $\Delta b_j(n)$ are the change in thresholds of the output, hidden and input layer respectively. The change in threshold is represented as,

$$\Delta b_l(n) = -2\mu \frac{\partial \xi(n)}{\partial b_l(n)} = \mu e(n) \frac{dy_l(n)}{db_l(n)}$$

$$= \mu e(n) \varphi_l' \left[\sum_{k=1}^{P_2} w_{kl} f_k + b_l\right] \quad (5.16)$$

From the structural point of MLP, it is very complex and it there are more than two hidden layers the structure becomes more complex. As more number of weights are present when implemented in DSP or FPGA memory requirements are considered and during updation of weights in Back Propagation it becomes very complex thereby causing over burden on the processor used. So a very simple and powerful structure is required and thus FLANN is considered.

In this study, we use the back-propagation network, that is, a multi-layer feed-forward neural network topology with one hidden-layer as shown in Figure 5.4. The feed forward back propagation (BP) network is a very popular model in neural networks. In multilayer feed forward networks, the processing elements are arranged in layers and only the elements

in adjacent layers are connected. It has minimum three layers of elements (i) the input layer (ii) the middle or hidden layer and (iii) the output layer. The name back propagation derives from the fact that computations are passed forward from the input to output layer, following which calculated errors are propagated back in the other direction to change the weights to obtain better performance. Back-propagation networks can be learned when presented with input-target output pairs.

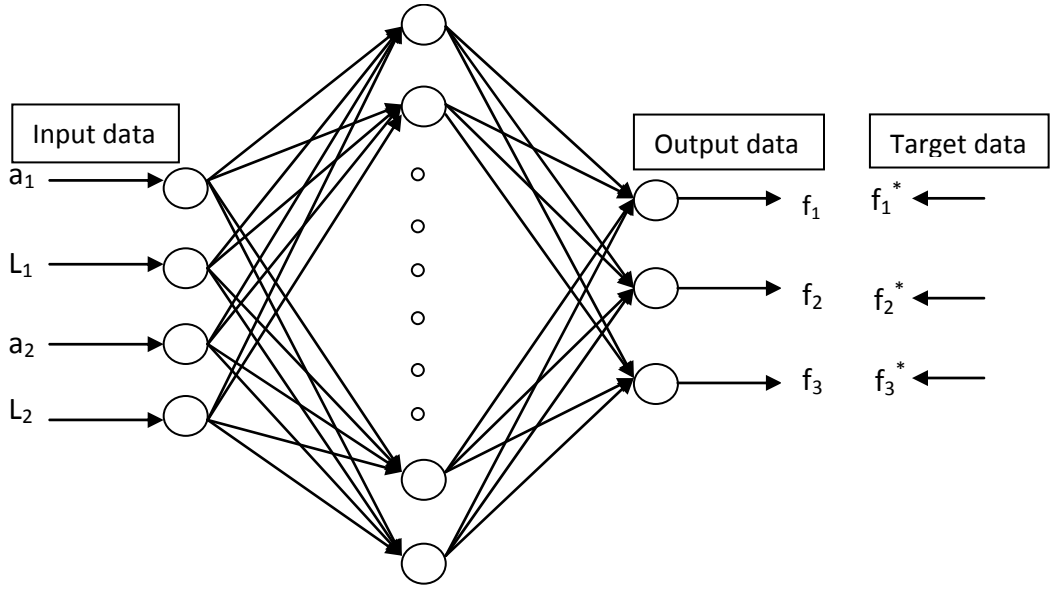

Fig.5.4 Three-layer neural network utilized in this study.

5.3 NEURAL NETWORK TRAINING

The clamped-free beam of Figure 4.1 has a length of L=0.8 m, width of the beam = 0.05 m, depth of the beam = 0.006 m, the material properties are E = 0.724×10^{11} N/m^2, Poisson's ratio = 0.334, ρ= 2713 kg/m^3. For the preparation of the learning data, 10 sets of a crack depths $a_1=a_2=0.0003,....,\ 0.003$m (step size=0.0003m) are introduced at the 17 different crack locations $L_1=0.04,....,\ 0.68$m (step size=0.04m) and $L_2=0.08,...,0.72$m (step size=0.04m). Totally 170 cases or patterns (10 different crack depths and 17different crack

locations) are solved for the first three frequencies. The patterns which consist of 170 sets of data are used to train the neural network of Figure5.5.

Because of the nature of the sigmoid activation function, i.e., saturation function, the output variables should be scaled by the user, to be within the most active range of the sigmoid function. Scaling rule that minimum and maximum values are set to 0.1 and 0.9 is usually suggested. Through some trials, a network with neuron arrangement (input-hidden-output) of 4-13-3 trained with 8 iteration for the 170 patterns are concluded to be the best for our application.

Mean-square error (MSE) is employed as a measurement of modelling performance. The mathematical expression can be described as follows:

$$\text{MSE} = \frac{\sum_{i=1}^{N} (e_i)^2}{N} \tag{5.17}$$

Where e_i denotes an error at pattern i and N is the total number of patterns.

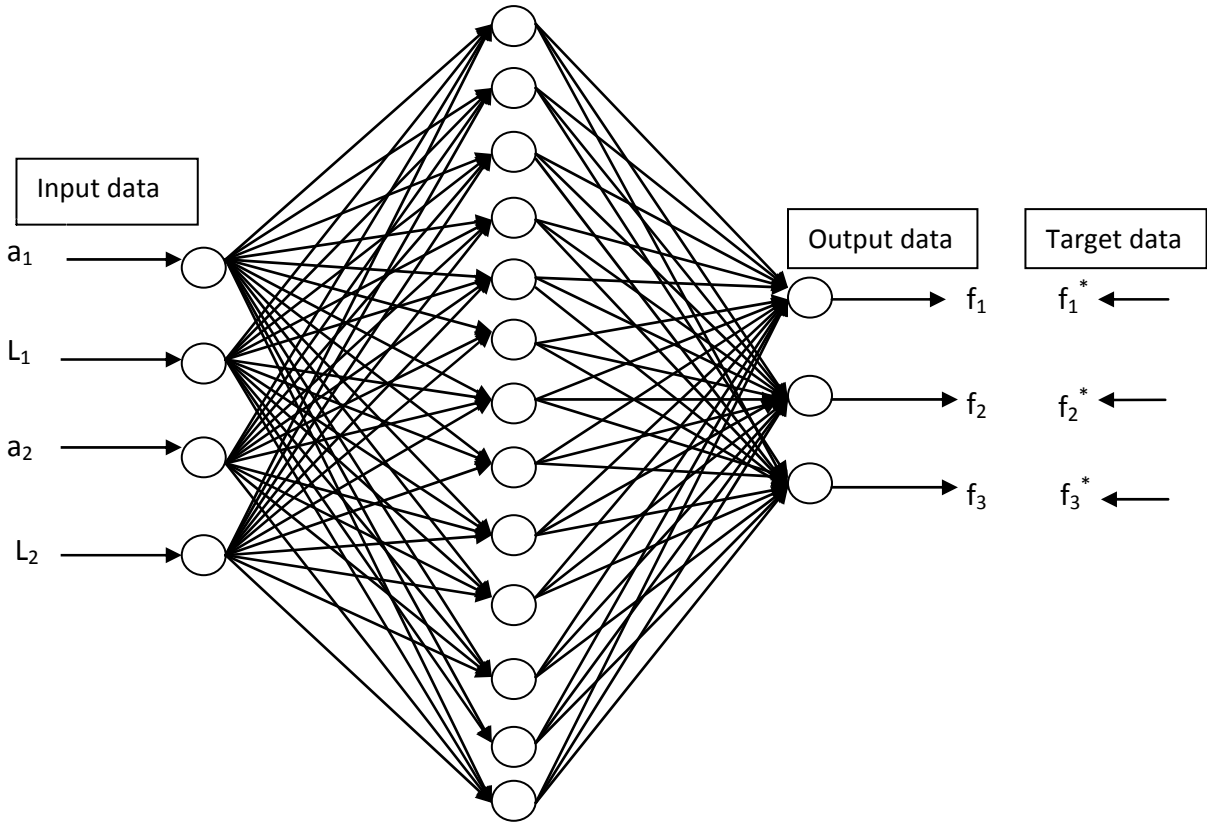

Figure 5.5.Three-layer neural network with neuron arrangement of 4-13-3.

CHAPTER 6

RESULTS & DISCUSSION

6. RESULTS AND DISCUSSION

6.1 NUMERICAL RESULTS

PROBLEM DEFINITION

The problem involves calculation of natural frequencies and mode shapes for cantilever beam without a crack and with two cracks of different crack depths. The results calculated analytically are validated with the results obtained by simulation analysis.

The method described has been applied to a cracked Bernoulli-Euler beam. Aluminum has taken the beam.

Properties:

Width of the beam = 0.05 m

Depth of the beam = 0.006 m

Length of the beam = 0.8 m

Elastic modulus of the beam = 0.724×10^{11} N/m^2

Poisson's Ratio = 0.334

Density = 2713 kg/m^3

End condition of the beam = One end fixed and other end free (Cantilever beam).

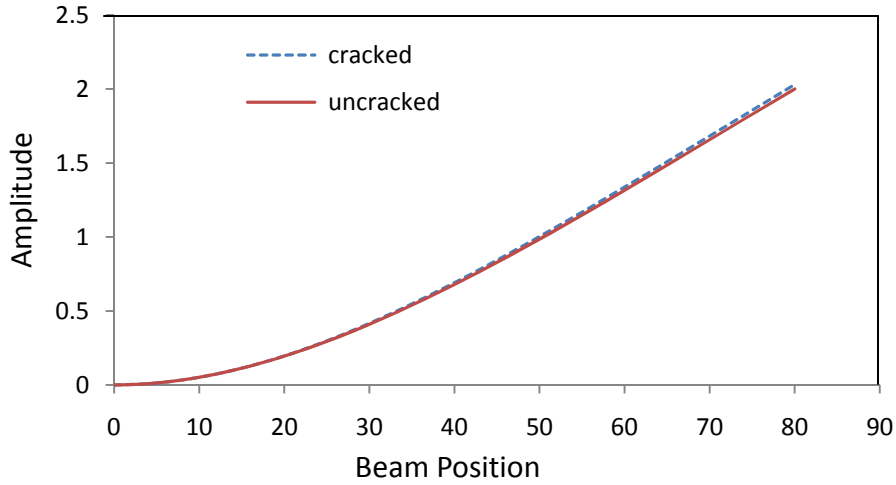

Fig.6.1. First mode of transverse vibration,

$a_1/w=0.1667$, $a_2/w=0.1667$, L1/L=0.125, L2/L=0.25

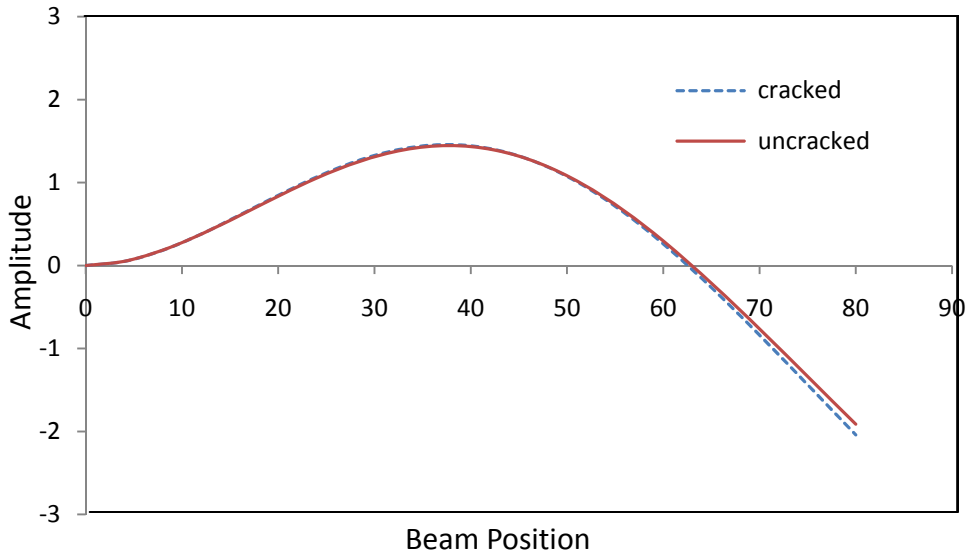

Fig.6.2. Second mode of transverse vibration,
a_1/w= 0.1667, a_2 /w=0.1667, L1/L=0.125, L2/L=0.25

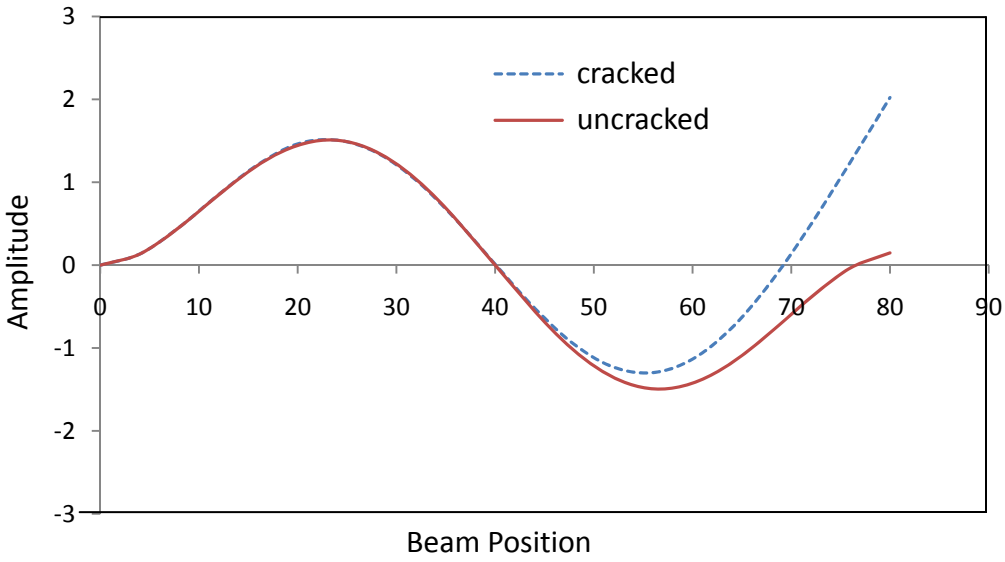

Fig.6.3. Third mode of transverse vibration,
a_1/w= 0.1667, a_2 /w=0.1667, L1/L=0.125, L2/L=0.25

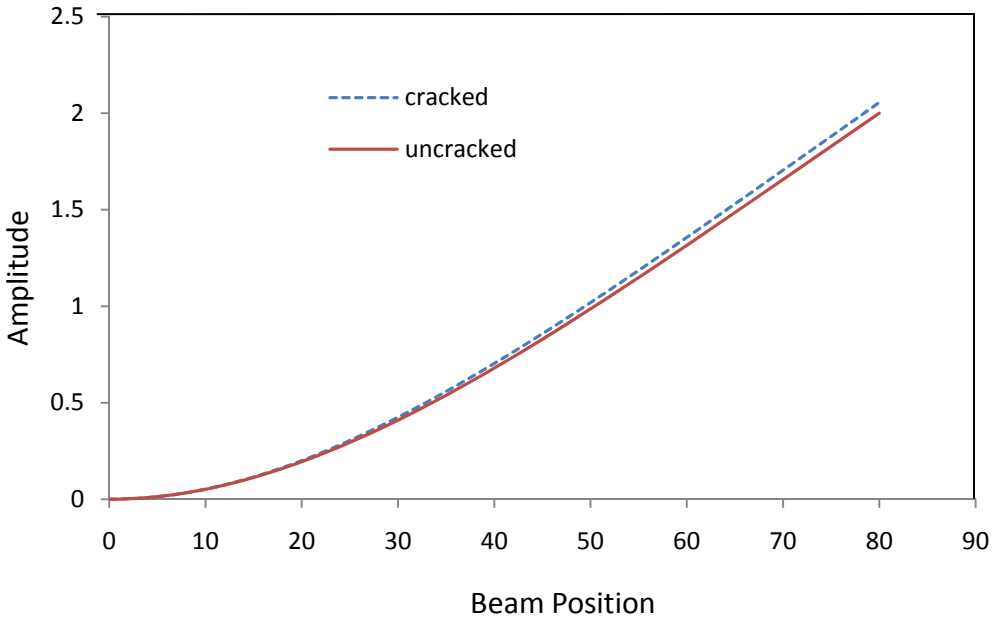

Fig.6.4. First mode of transverse vibration,
$a_1/w=0.334$, $a_2/w=0.334$, L1/L=0.125, L2/L=0.25

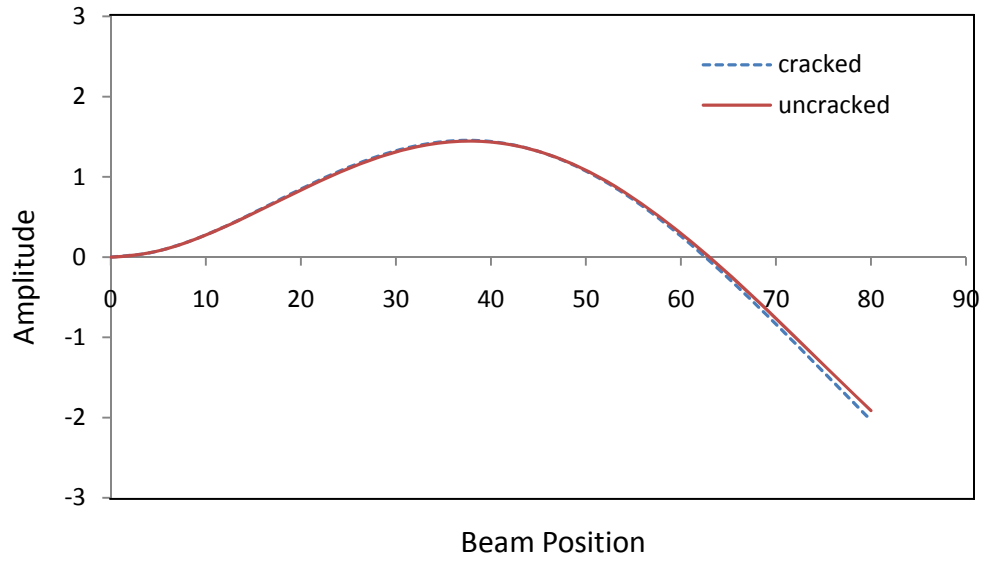

Fig.6.5. Second mode of transverse vibration,
$a_1/w=0.334$, $a_2/w=0.334$, L1/L=0.125, L2/L=0.25

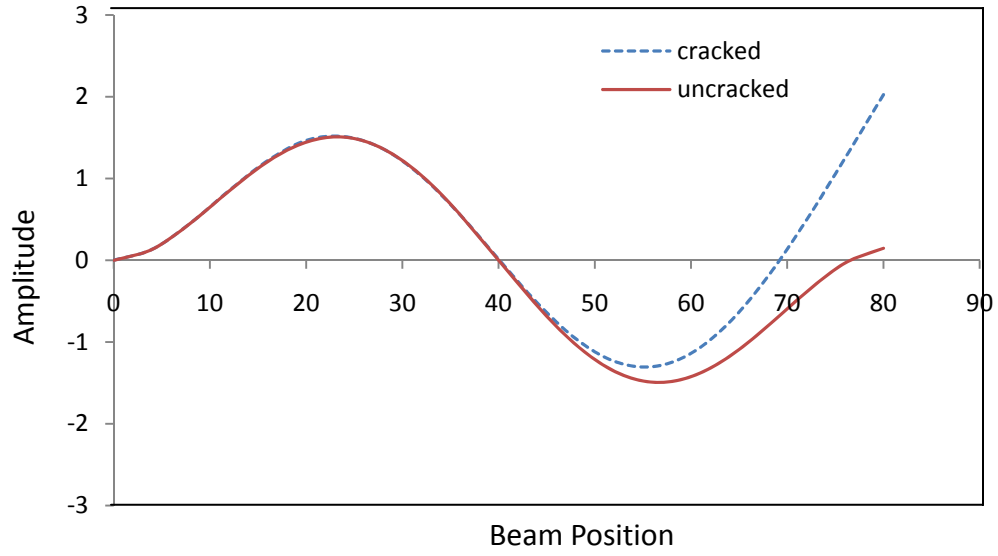

Fig.6.6. Third mode of transverse vibration,
$a_1/w=0.334$, $a_2/w=0.334$, L1/L=0.125, L2/L=0.25

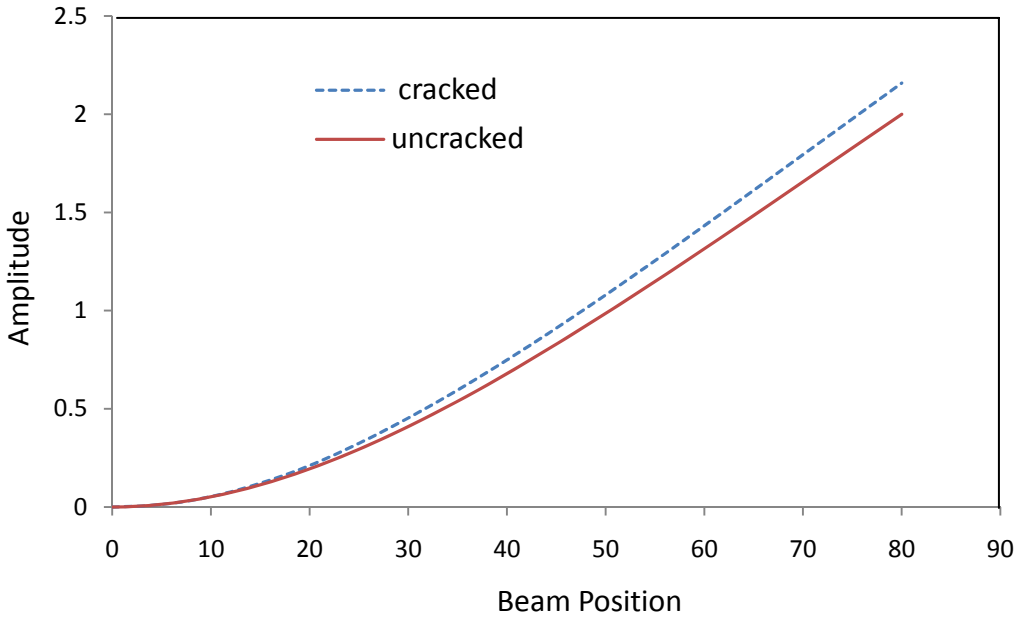

Fig.6.7. First mode of transverse vibration,
$a_1/w=0.5$, $a_2/w=0.5$, L1/L=0.125, L2/L=0.25

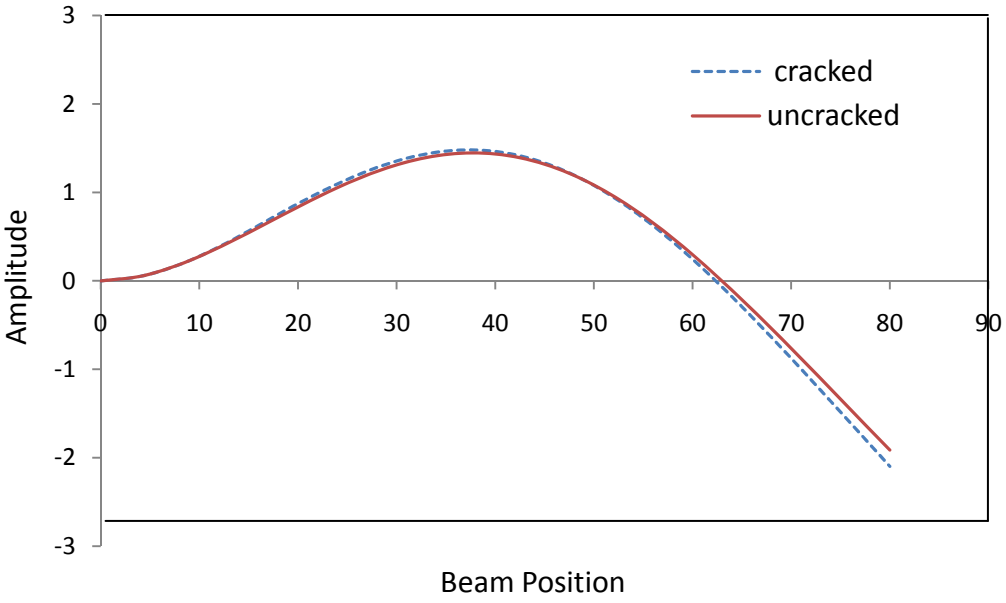

Fig.6.8. Second mode of transverse vibration, $a_1/w=0.5$, $a_2/w=0.5$, L1/L=0.125, L2/L=0.25

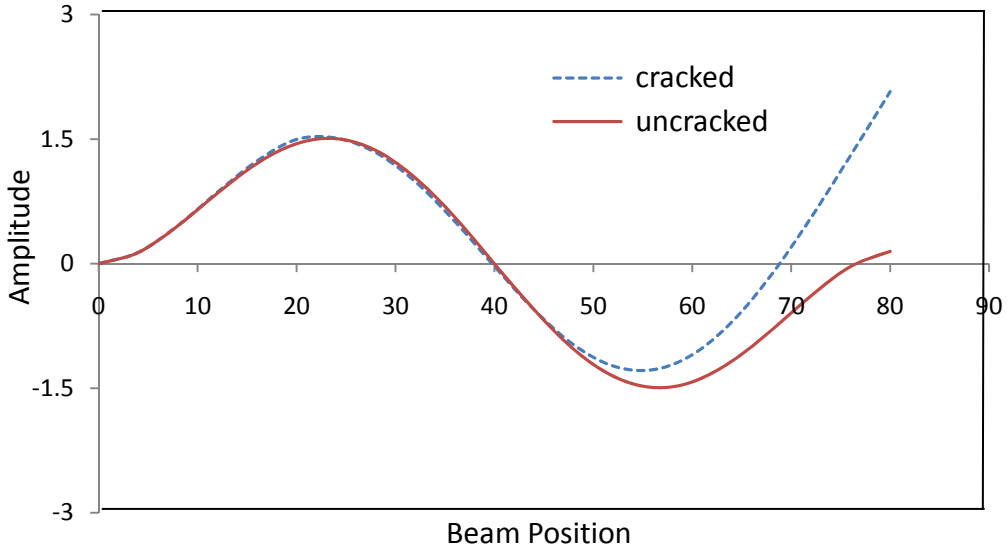

Fig.6.9. Third mode of transverse vibration, $a_1/w=0.5$, $a_2/w=0.5$,L1/L=0.125, L2/L=0.25

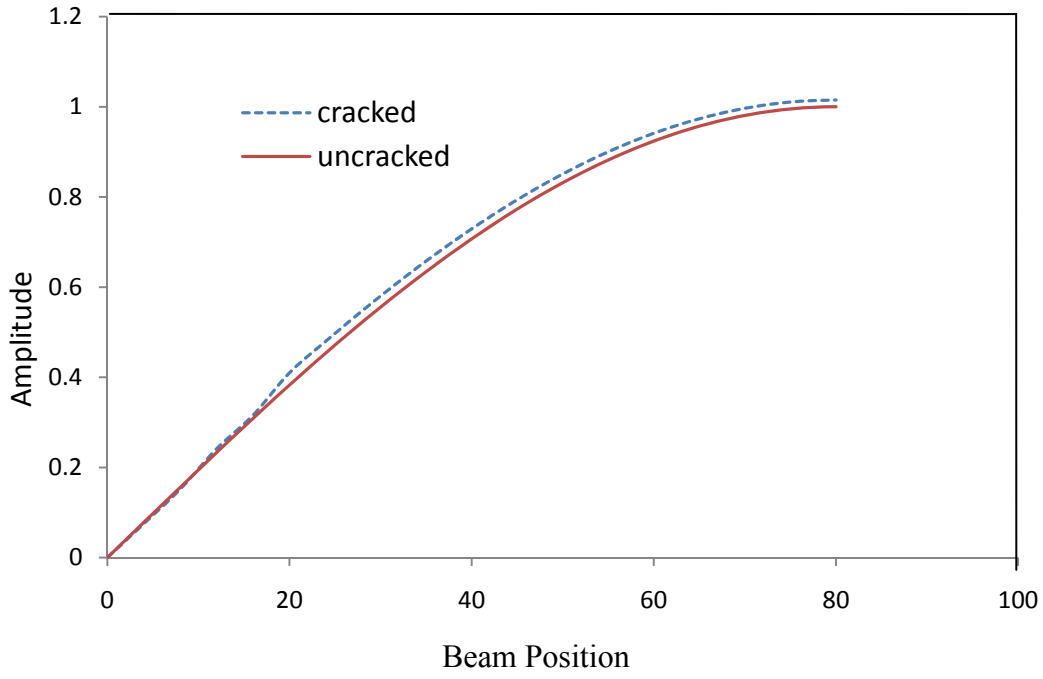

Fig.6.10. First mode of longitudinal vibration,
a_1/w=0.1667, a_2 /w=0.1667, L1/L=0.125, L2/L=0.25

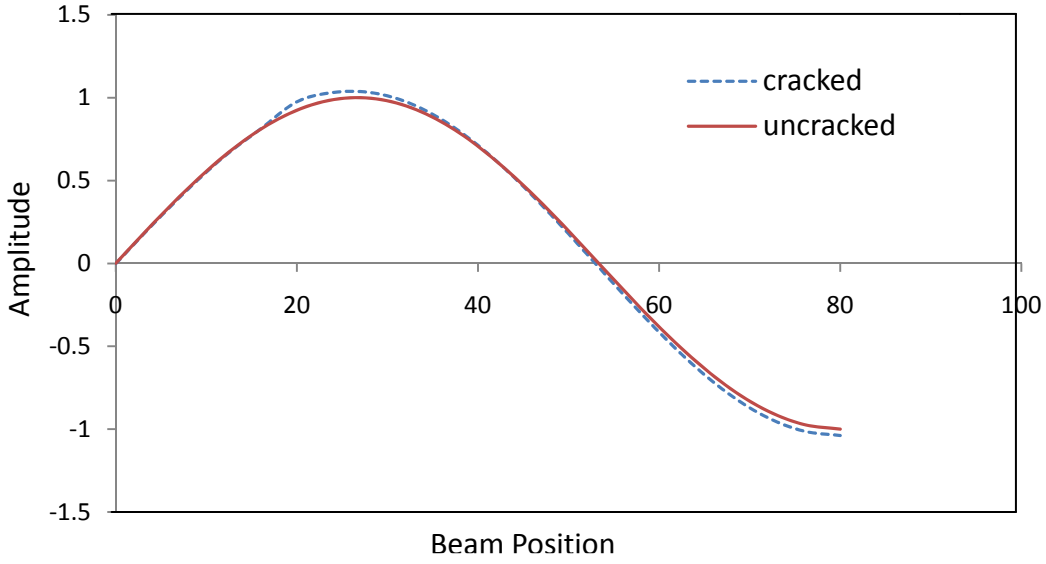

Fig.6.11. Second mode of longitudinal vibration,
a_1/w= 0.1667, a_2 /w=0.1667, L1/L=0.125, L2/L=0.25

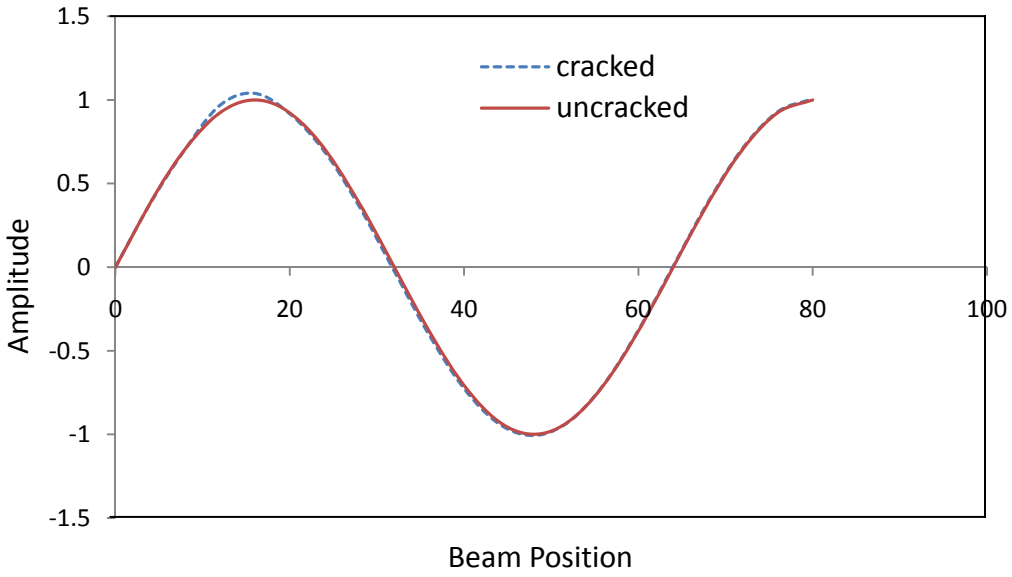

Fig.6.12. Third mode of longitudinal vibration,
a_1/w= 0.1667, a_2 /w=0.1667, L1/L=0.125, L2/L=0.25

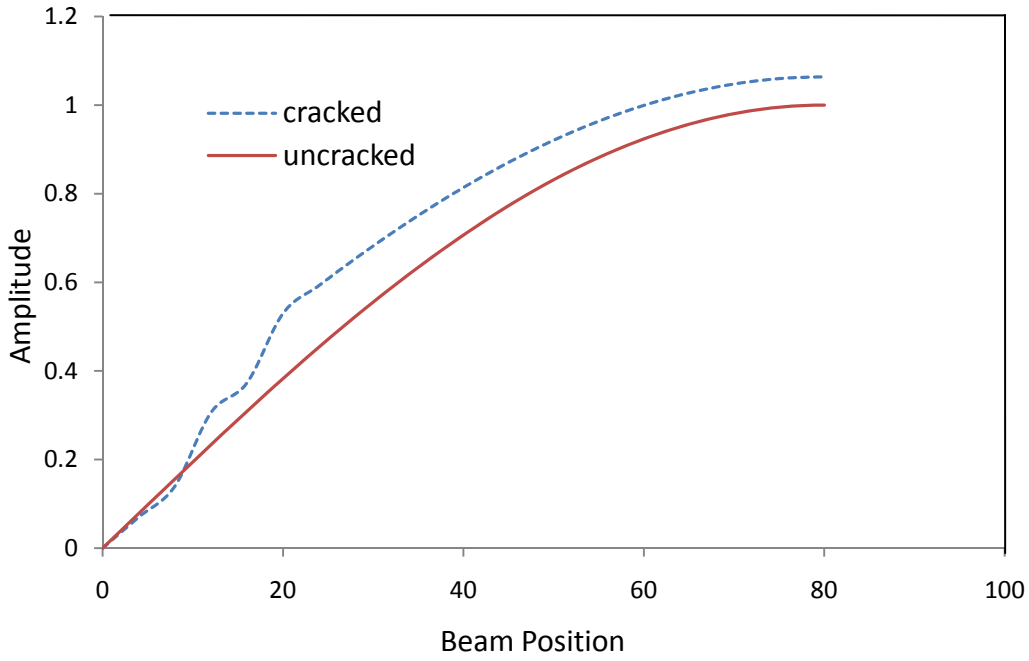

Fig.6.13. First mode of longitudinal vibration,
a_1/w= 0.334, a_2 /w=0.334, L1/L=0.125, L2/L=0.25

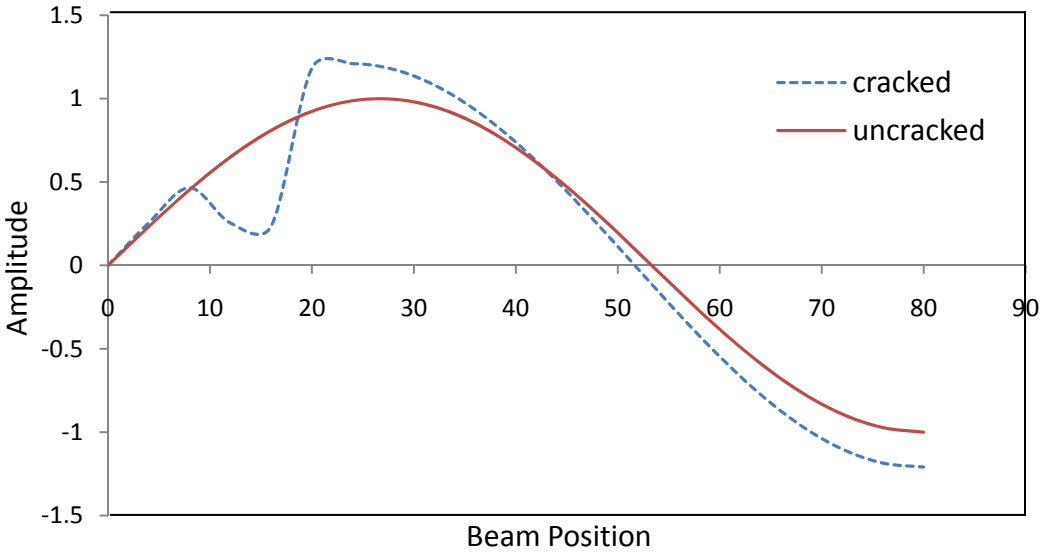

Fig.6.14. Second mode of longitudinal vibration,
$a_1/w=0.334$, $a_2/w=0.334$, L1/L=0.125, L2/L=0.25

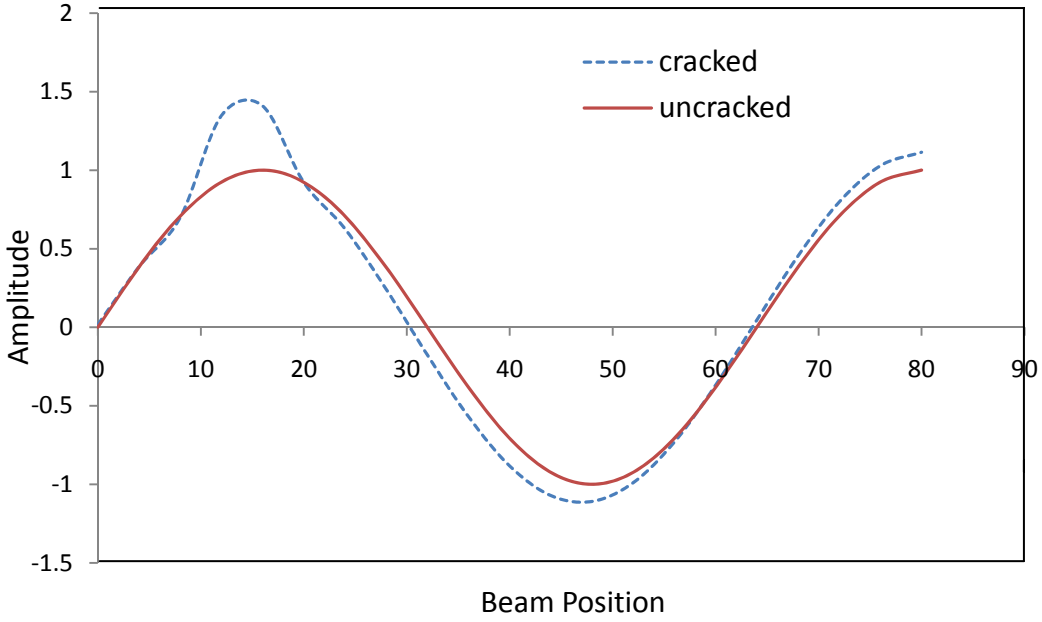

Fig.6.15. Third mode of longitudinal vibration,
$a_1/w=0.334$, $a_2/w=0.334$, L1/L=0.125, L2/L=0.25

6.2. SIMULATION RESULTS

6.2.1 MODAL ANALYSIS

Following steps show the guidelines for carrying out Modal analysis.

Define Materials

1. Set preferences. (Structural)
2. Define constant material properties.

Model the Geometry

3. Follow bottom up modeling and create the geometry

Generate Mesh

4. Define element type.
5. Mesh the area.

Apply Boundary Conditions

6. Apply constraints to the model.

Obtain Solution

7. Specify analysis types and options.
8. Solve.

6.2.2 Finite element modeling

The ANSYS 10.0 finite element program was used for free vibration of the cracked beams. For this purpose, the key points were first created and then line segments were formed. The lines were combined to create an area. Finally, this area was extruded and a three-dimensional V-shaped edge cracked beam model was obtained. We modeled the crack with a 0.5mm width on the top surface of the beam and a crack going through the depth of the beam. A 20-node three-dimensional structural solid element under SOLID 95 was selected to model the beam. The beam was discretized into 1045 elements with 2318 nodes. Cantilever boundary conditions can also be modeled by constraining all degrees of freedoms of the nodes located on the left end of the beam. The subspace mode extraction method was used to calculate the natural frequencies of the beam. The subspace mode extraction method was used to calculate the natural frequencies of the beam.

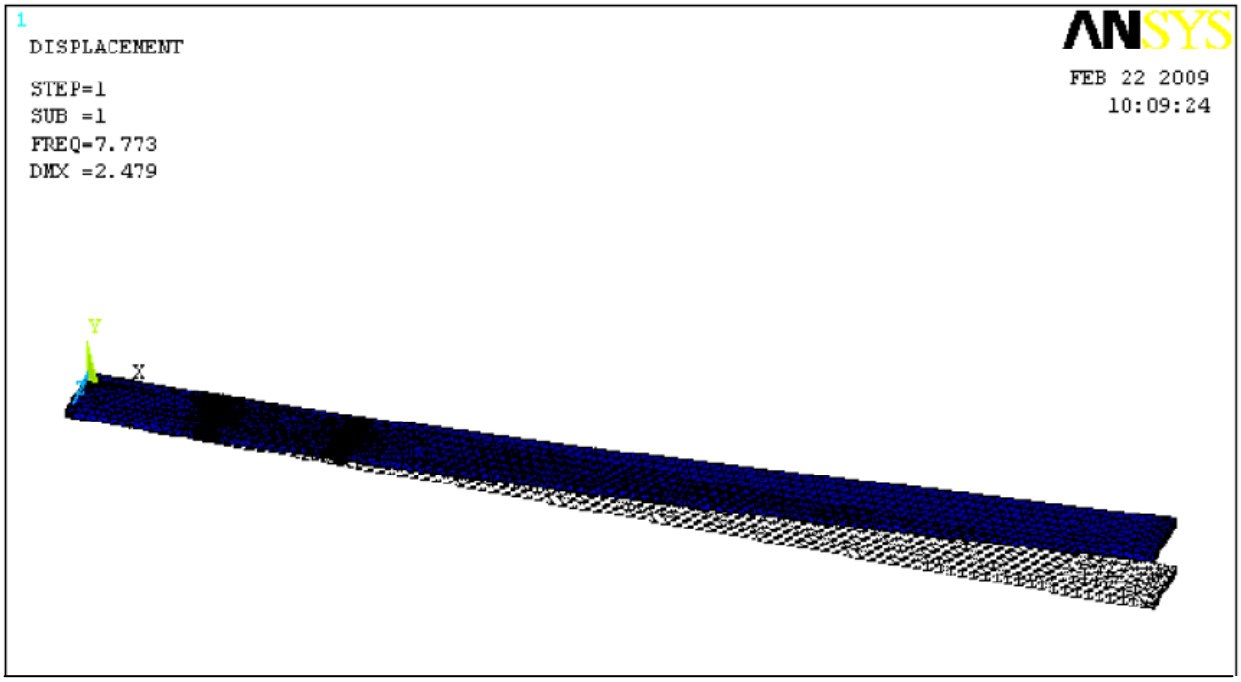

Fig.6.21. First mode of vibration, $a_1/w=0.1667$, $a_2/w=0.1667$, $L_1/L=0.125$, $L_2/L=0.25$.

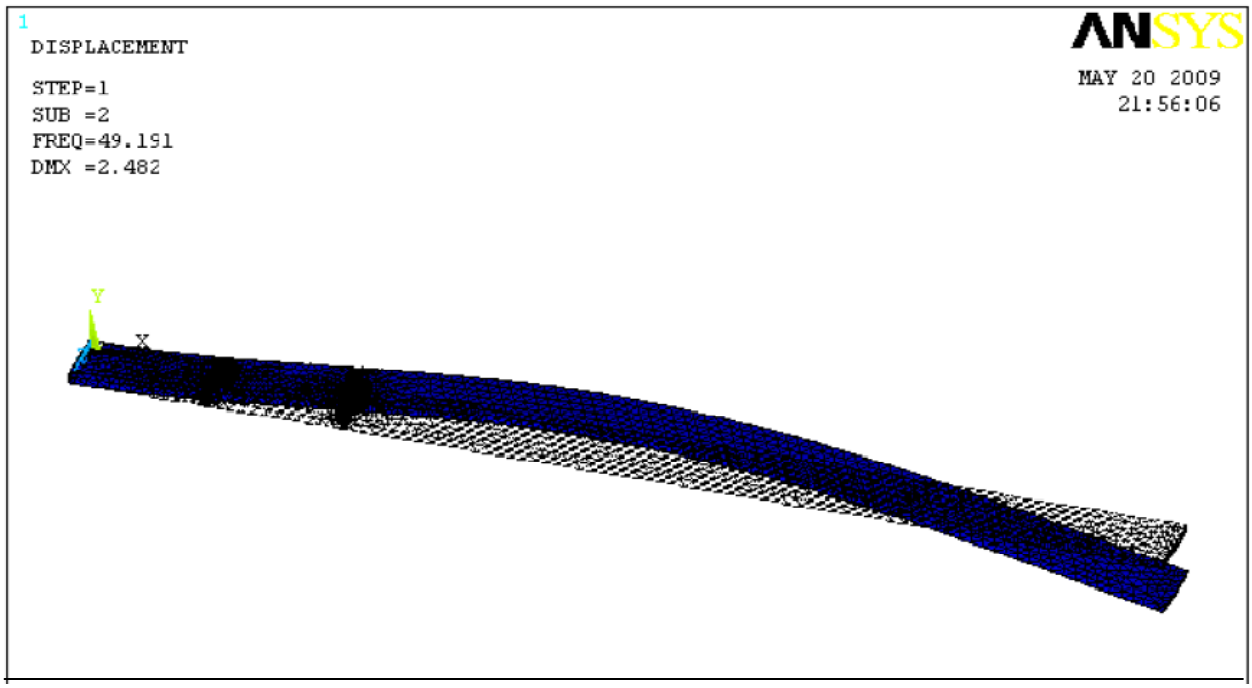

Fig.6.22. Second mode of vibration, $a_1/w=0.1667$, $a_2/w=0.1667$, $L_1/L=0.125$, $L_2/L=0.25$.

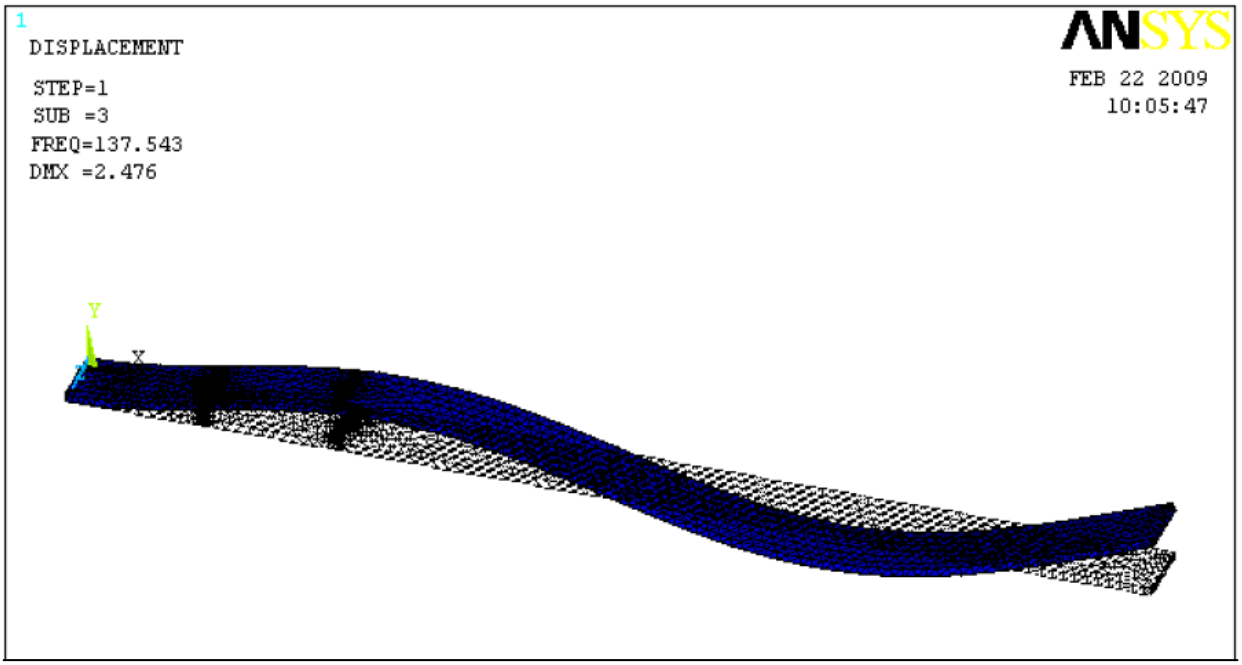

Fig.6.23. Third mode of vibration, $a_1/w=0.1667$, $a_2/w=0.1667$, $L_1/L=0.125$, $L_2/L=0.25$.

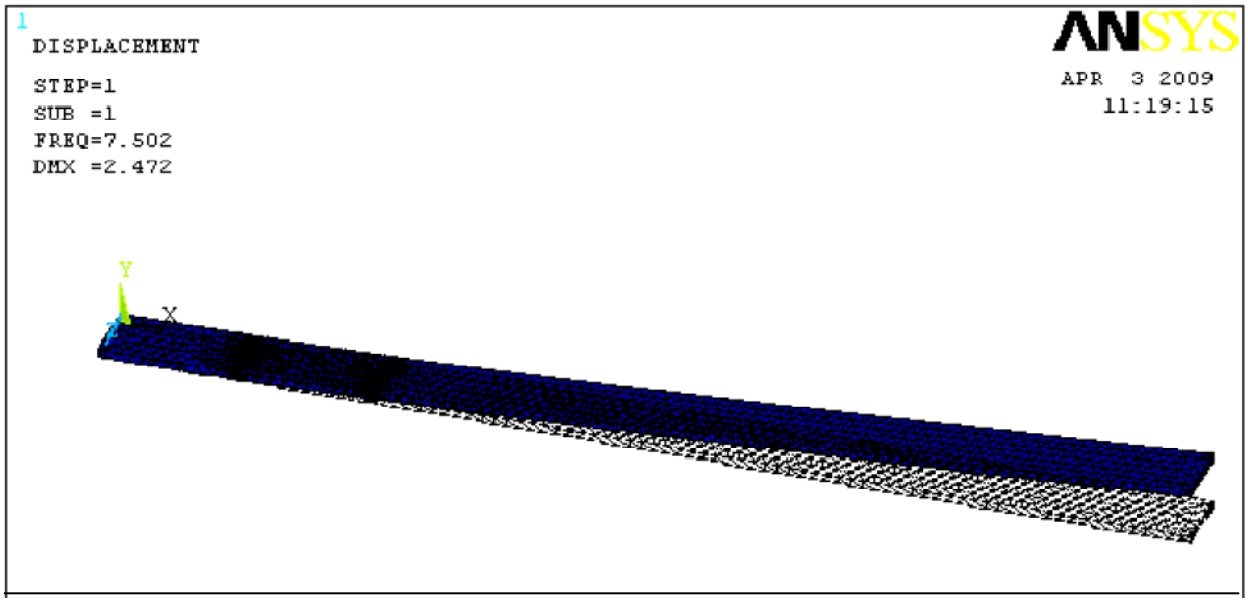

Fig.6.24. First mode of vibration, $a_1/w=0.334$, $a_2/w=0.334$, $L_1/L=0.125$, $L_2/L=0.25$.

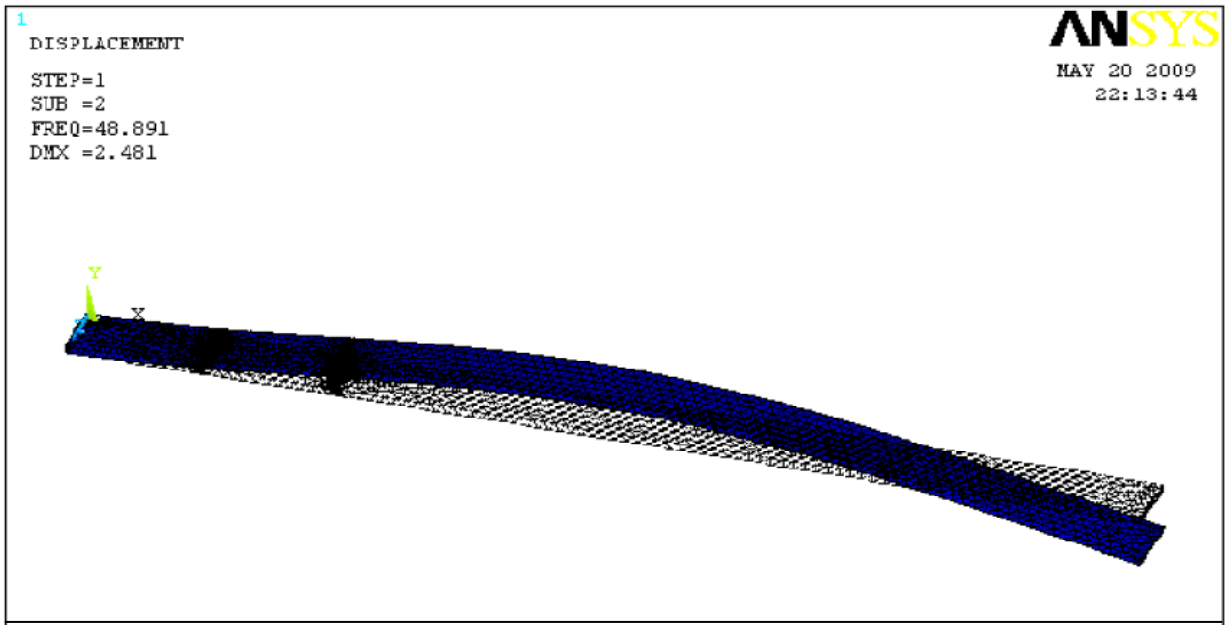

Fig.6.25. Second mode of vibration, $a_1/w=0.334$, $a_2/w=0.334$, $L_1/L=0.125$, $L_2/L=0.25$.

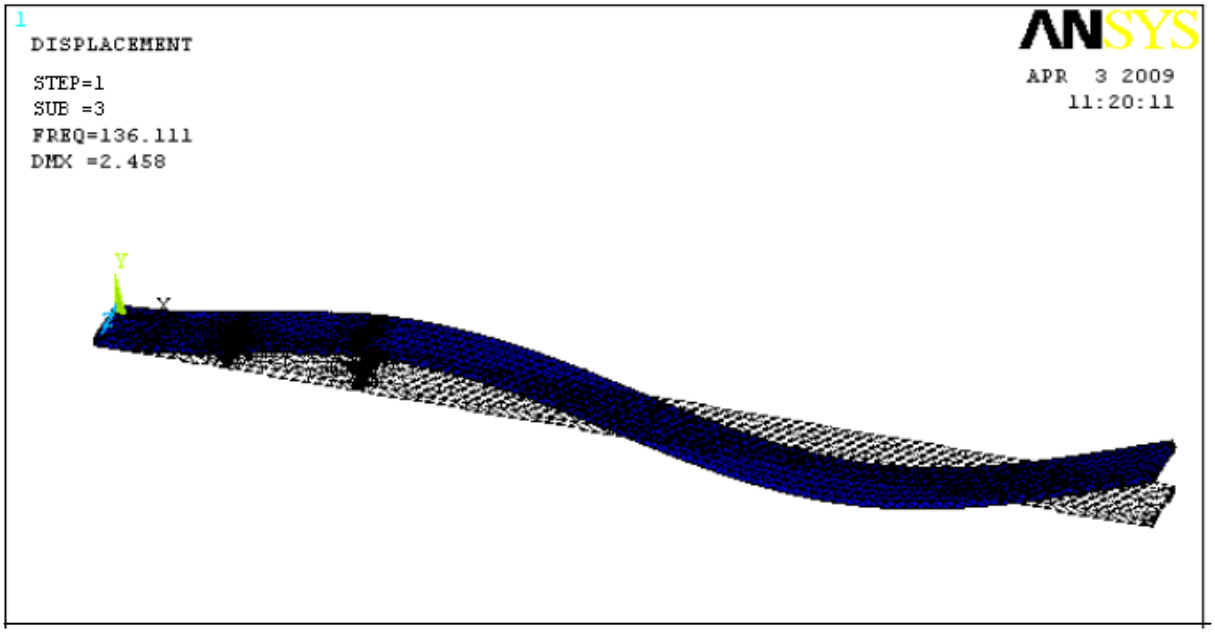

Fig.6.26. Third mode of vibration, $a_1/w=0.334$, $a_2/w=0.334$, $L_1/L=0.125$, $L_2/L=0.25$.

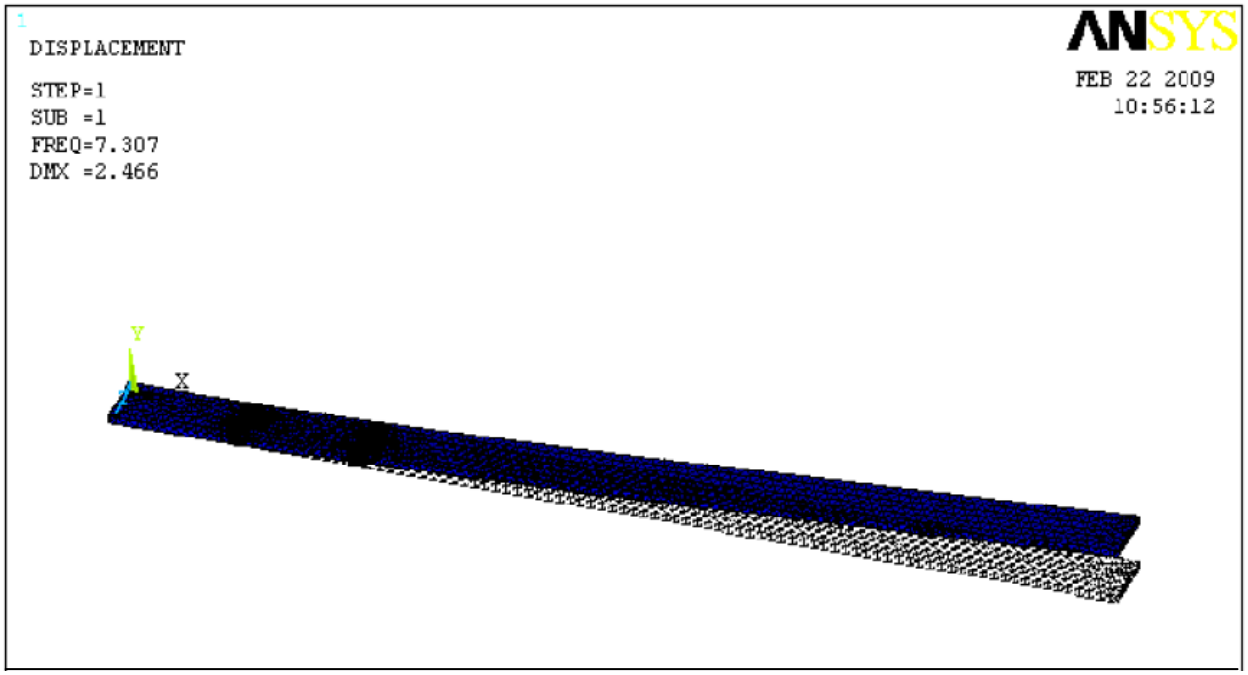

Fig.6.27. First mode of vibration, $a_1/w=0.5$, $a_2/w=0.5$, $L_1/L=0.125$, $L_2/L=0.25$.

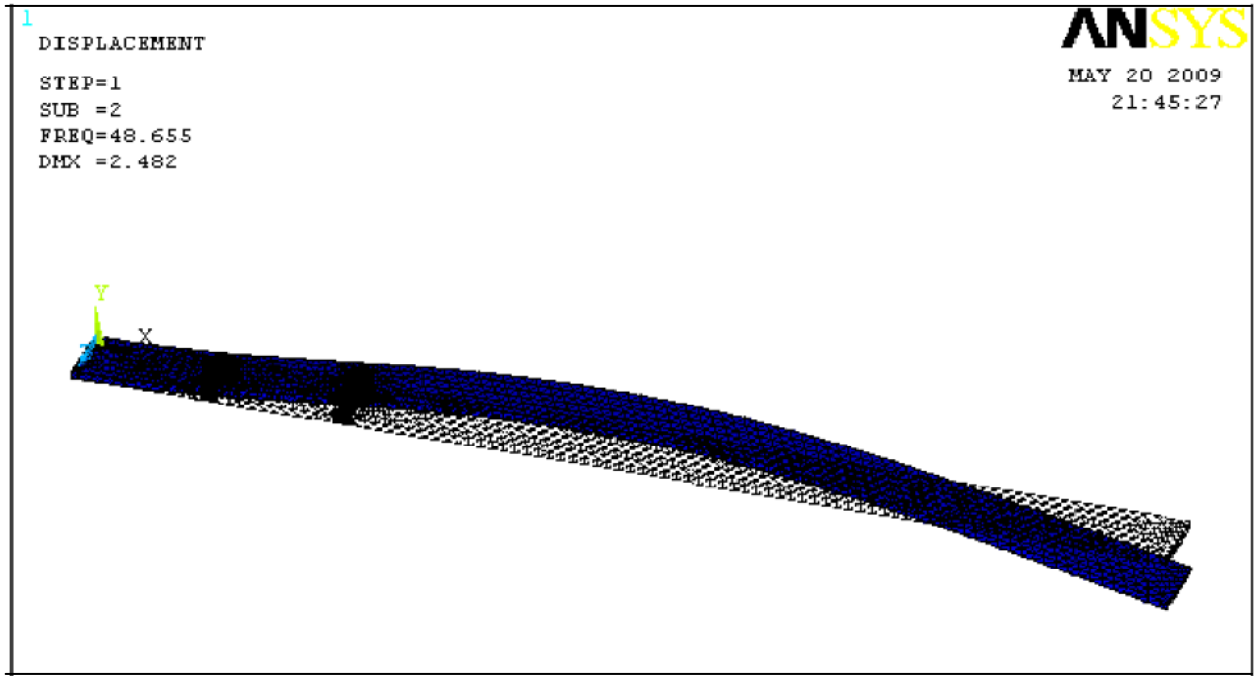

Fig.6.28. Second mode of vibration,$a_1/w=0.5$, $a_2/w=0.5$, $L_1/L=0.125$, $L_2/L=0.25$.

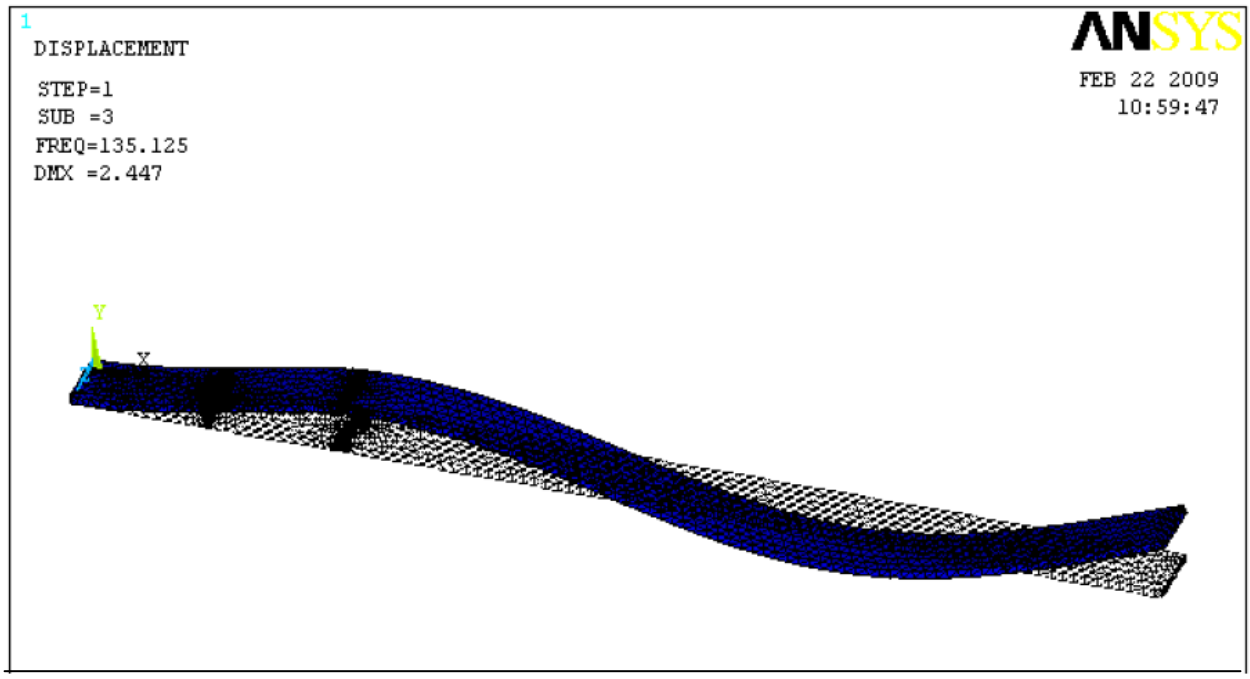

Fig. 6.29.Third mode of vibration, $a_1/w=0.5$, $a_2/w=0.5$, $L_1/L=0.125$, $L_2/L=0.25$.

Table 6.1. Variation of frequencies at different Relative crack depths when Relative Crack location at $L_1/L=0.125$, $L_2/L=0.25$.

Relative crack depth	Frequency first mode HZ	Frequency Found in ANSYS HZ	Frequency second mode HZ	Frequency Found in ANSYS HZ	Frequency Third mode HZ	Frequency Found in ANSYS HZ
0.08335	7.754	7.844	49.220	49.263	137.812	137.902
0.1667	7.684	7.773	49.119	49.191	137.452	137.543
0.250	7.588	7.631	48.950	49.045	136.651	136.744
0.334	7.463	7.502	48.825	48.891	135.980	136.111
0.5	7.285	7.307	48.573	48.655	134.931	135.125
0.667	6.988	7.059	48.266	48.346	133.050	133.225
0.8	6.553	6.642	47.719	47.791	131.216	131.398

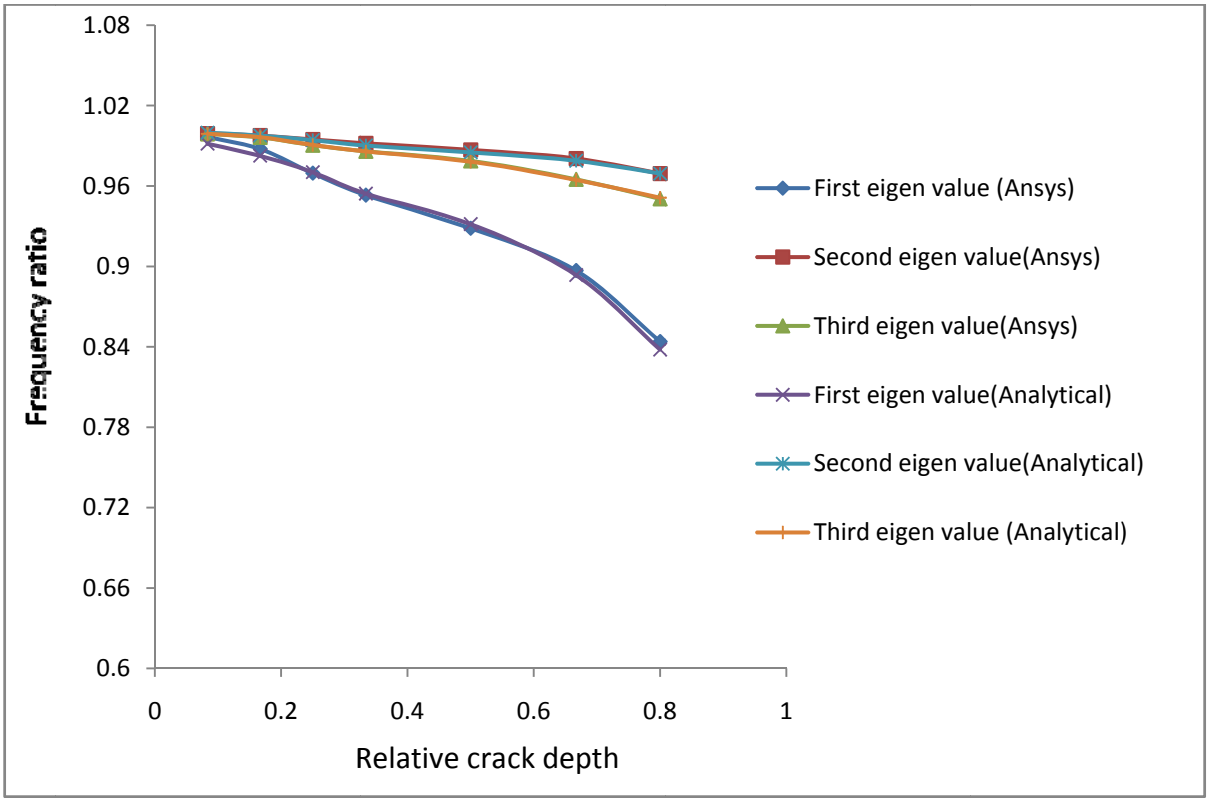

Fig.6.33. Frequency ratio vs Relative crack depth at $L_1/L=0.125$, $L_2/L=0.25$.

6.3 Neural Network Training

Table 6.3. Neural Network Training Data (170Patterns)

Sr. No.	Crack depth ($a_1 = a_2$) m	L_1 m	L_2 m	f_1 Hz	f_2 Hz	f_3 Hz
1	0.0003	0.04	0.08	7.8668	49.293	138.04
2		0.08	0.12	7.8678	49.302	138.06
3		0.12	0.16	7.8683	49.306	138.06
4		0.16	0.2	7.8682	49.305	138.05
5		0.2	0.24	7.8671	49.296	138.02
6		0.24	0.28	7.8694	49.306	138.05
7		0.28	0.32	7.8686	49.297	138.03
8		0.32	0.36	7.8697	49.300	138.06
9		0.36	0.4	7.8889	49.292	138.05
10		0.4	0.44	7.8702	49.298	138.06
11		0.44	0.48	7.8699	49.296	138.05
12		0.48	0.52	7.8702	49.298	138.04
13		0.52	0.56	7.8706	49.301	138.04
14		0.56	0.6	7.8699	49.299	138.02
15		0.6	0.64	7.8701	49.301	138.03
16		0.64	0.68	7.8697	49.300	138.03
17		0.68	0.72	7.8697	49.301	138.04

Sr. No.	Crack depth ($a_1 = a_2$) m	L_1 m	L_2 m	f_1 Hz	f_2 Hz	f_3 Hz
1	0.0006	0.04	0.08	7.8591	49.269	138.01
2		0.08	0.12	7.8594	49.284	138.04
3		0.12	0.16	7.8602	49.292	138.02
4		0.16	0.2	7.8635	49.306	138.01
5		0.2	0.24	7.8644	49.303	137.97
6		0.24	0.28	7.8646	49.287	137.95
7		0.28	0.32	7.8665	49.282	137.99
8		0.32	0.36	7.8679	49.276	138.03
9		0.36	0.4	7.8683	49.266	138.05
10		0.4	0.44	7.8683	49.259	138.04
11		0.44	0.48	7.8690	49.261	138.01
12		0.48	0.52	7.8689	49.265	137.96
13		0.52	0.56	7.8690	49.272	137.92
14		0.56	0.6	7.8692	49.278	137.91
15		0.6	0.64	7.8706	49.295	137.95
16		0.64	0.68	7.8703	49.298	137.98
17		0.68	0.72	7.8702	49.301	138.02

Sr. No.	Crack depth ($a_1 = a_2$) m	L_1 m	L_2 m	f_1 Hz	f_2 Hz	f_3 Hz
1	0.0009	0.04	0.08	7.8443	49.215	137.92
2		0.08	0.12	7.8458	49.256	137.01
3		0.12	0.16	7.8497	49.287	137.99
4		0.16	0.2	7.8545	49.302	137.93
5		0.2	0.24	7.8577	49.296	137.86
6		0.24	0.28	7.8595	49.274	137.83
7		0.28	0.32	7.8617	49.250	137.89
8		0.32	0.36	7.8636	49.228	137.97
9		0.36	0.4	7.8656	49.215	137.03
10		0.4	0.44	7.8651	49.196	138.00
11		0.44	0.48	7.8685	49.214	137.97
12		0.48	0.52	7.8678	49.218	137.84
13		0.52	0.56	7.8701	49.242	137.78
14		0.56	0.6	7.8704	49.262	137.77
15		0.6	0.64	7.8706	49.279	137.82
16		0.64	0.68	7.8697	49.286	137.89
17		0.68	0.72	7.8697	49.294	137.97

Sr. No.	Crack depth ($a_1 = a_2$) m	L_1 m	L_2 m	f_1 Hz	f_2 Hz	f_3 Hz
1	0.0012	0.04	0.08	7.8268	49.159	137.85
2		0.08	0.12	7.8307	49.233	138.01
3		0.12	0.16	7.8383	49.291	137.99
4		0.16	0.2	7.8431	49.303	137.84
5		0.2	0.24	7.8499	49.293	137.74
6		0.24	0.28	7.8520	49.251	137.67
7		0.28	0.32	7.8546	49.202	137.74
8		0.32	0.36	7.8593	49.176	137.91
9		0.36	0.4	7.8618	49.145	137.01
10		0.4	0.44	7.8655	49.139	137.03
11		0.44	0.48	7.8667	49.144	137.90
12		0.48	0.52	7.8681	49.165	137.72
13		0.52	0.56	7.8699	49.194	137.57
14		0.56	0.6	7.8702	49.229	137.55
15		0.6	0.64	7.8702	49.257	137.63
16		0.64	0.68	7.8693	49.273	137.76
17		0.68	0.72	7.8700	49.291	137.92

Sr. No.	Crack depth ($a_1 = a_2$) m	L_1 m	L_2 m	f_1 Hz	f_2 Hz	f_3 Hz
1	0.0015	0.04	0.08	7.7981	49.062	137.71
2		0.08	0.12	7.8079	49.201	138.01
3		0.12	0.16	7.8181	49.272	137.92
4		0.16	0.2	7.8276	49.296	137.70
5		0.2	0.24	7.8351	49.278	137.49
6		0.24	0.28	7.8425	49.223	137.46
7		0.28	0.32	7.8497	49.166	137.63
8		0.32	0.36	7.8536	49.094	137.84
9		0.36	0.4	7.8587	49.058	138.02
10		0.4	0.44	7.8620	49.036	138.00
11		0.44	0.48	7.8652	49.054	137.81
12		0.48	0.52	7.8667	49.080	137.52
13		0.52	0.56	7.8690	49.132	137.30
14		0.56	0.6	7.8701	49.183	137.24
15		0.6	0.64	7.8699	49.227	137.37
16		0.64	0.68	7.8718	49.275	137.66
17		0.68	0.72	7.8721	49.299	137.89

Sr. No.	Crack depth ($a_1 = a_2$) m	L_1 m	L_2 m	f_1 Hz	f_2 Hz	f_3 Hz
1	0.0018	0.04	0.08	7.7674	48.959	137.56
2		0.08	0.12	7.7809	49.155	137.99
3		0.12	0.16	7.7944	49.268	137.90
4		0.16	0.2	7.8087	489.296	137.55
5		0.2	0.24	7.8205	49.264	137.25
6		0.24	0.28	7.8306	49.188	137.20
7		0.28	0.32	7.8388	49.093	137.40
8		0.32	0.36	7.8469	49.010	137.75
9		0.36	0.4	7.8528	48.943	137.99
10		0.4	0.44	7.8574	48.900	137.96
11		0.44	0.48	7.8610	48.924	137.67
12		0.48	0.52	7.8653	48.969	137.25
13		0.52	0.56	7.88681	49.049	137.95
14		0.56	0.6	7.8700	49.132	137.90
15		0.6	0.64	7.8704	49.200	137.10
16		0.64	0.68	7.8718	49.257	137.45
17		0.68	0.72	7.8710	49.284	137.78

Sr. No.	Crack depth ($a_1 = a_2$) m	L_1 m	L_2 m	f_1 Hz	f_2 Hz	f_3 Hz
1	0.0021	0.04	0.08	7.7269	48.826	137.37
2		0.08	0.12	7.7500	49.103	137.96
3		0.12	0.16	7.7668	49.257	137.83
4		0.16	0.2	7.7844	49.293	137.90
5		0.2	0.24	7.7997	49.247	136.92
6		0.24	0.28	7.8138	49.138	136.84
7		0.28	0.32	7.8254	49.00	137.13
8		0.32	0.36	7.8375	48.886	137.63
9		0.36	0.4	7.8463	48.806	137.96
10		0.4	0.44	7.8524	48.752	137.93
11		0.44	0.48	7.8604	48.768	137.53
12		0.48	0.52	7.8613	48.820	136.89
13		0.52	0.56	7.8667	48.939	136.49
14		0.56	0.6	7.8691	49.059	136.43
15		0.6	0.64	7.8696	49.150	136.67
16		0.64	0.68	7.8717	49.235	137.20
17		0.68	0.72	7.8725	49.285	137.69

Sr. No.	Crack depth ($a_1 = a_2$) m	L_1 m	L_2 m	f_1 Hz	f_2 Hz	f_3 Hz
1	0.0024	0.04	0.08	7.6730	48.650	137.12
2		0.08	0.12	7.7055	49.030	137.92
3		0.12	0.16	7.7321	49.231	137.73
4		0.16	0.2	7.7564	49.293	137.11
5		0.2	0.24	7.7777	49.232	136.57
6		0.24	0.28	7.7932	49.076	136.40
7		0.28	0.32	7.8102	48.897	136.81
8		0.32	0.36	7.8251	48.736	137.46
9		0.36	0.4	7.8361	48.596	137.92
10		0.4	0.44	7.8468	48.554	137.90
11		0.44	0.48	7.8554	48.605	137.36
12		0.48	0.52	7.8600	48.686	136.58
13		0.52	0.56	7.8644	48.802	135.92
14		0.56	0.6	7.8683	48.959	135.78
15		0.6	0.64	7.8702	49.104	136.21
16		0.64	0.68	7.8712	49.206	136.89
17		0.68	0.72	7.8720	49.272	137.55

Sr. No.	Crack depth ($a_1 = a_2$) m	L_1 m	L_2 m	f_1 Hz	f_2 Hz	f_3 Hz
1	0.0027	0.04	0.08	7.6200	48.479	136.891
2		0.08	0.12	7.6534	48.943	137.86
3		0.12	0.16	7.6849	48.202	137.62
4		0.16	0.2	7.7176	48.283	136.76
5		0.2	0.24	7.7454	48.206	136.05
6		0.24	0.28	7.7688	49.00	135.89
7		0.28	0.32	7.7907	48.762	136.42
8		0.32	0.36	7.8112	48.562	137.28
9		0.36	0.4	7.8246	48.372	137.86
10		0.4	0.44	7.8365	48.294	137.79
11		0.44	0.48	7.8501	48.367	137.12
12		0.48	0.52	7.8564	48.477	136.11
13		0.52	0.56	7.8634	48.652	135.30
14		0.56	0.6	7.8666	48.827	134.90
15		0.6	0.64	7.8687	48.029	135.60
16		0.64	0.68	7.8723	48.182	136.54
17		0.68	0.72	7.8724	48.262	137.39

Sr. No.	Crack depth ($a_1 = a_2$) m	L_1 m	L_2 m	f_1 Hz	f_2 Hz	f_3 Hz
1	0.003	0.04	0.08	7.5523	48.270	136.59
2		0.08	0.12	7.5899	48.844	137.80
3		0.12	0.16	7.6353	49.189	137.51
4		0.16	0.2	7.6737	49.273	136.39
5		0.2	0.24	7.7025	49.156	135.35
6		0.24	0.28	7.7414	48.916	135.32
7		0.28	0.32	7.7680	48.607	135.97
8		0.32	0.36	7.7928	49.323	137.06
9		0.36	0.4	7.8129	48.118	137.83
10		0.4	0.44	7.8288	48.031	137.75
11		0.44	0.48	7.8418	48.042	136.80
12		0.48	0.52	7.8630	48.737	136.30
13		0.52	0.56	7.8610	48.460	134.56
14		0.56	0.6	7.8658	48.717	134.29
15		0.6	0.64	7.8697	48.955	134.88
16		0.64	0.68	7.8724	49.140	136.03
17		0.68	0.72	7.8715	49.242	137.16

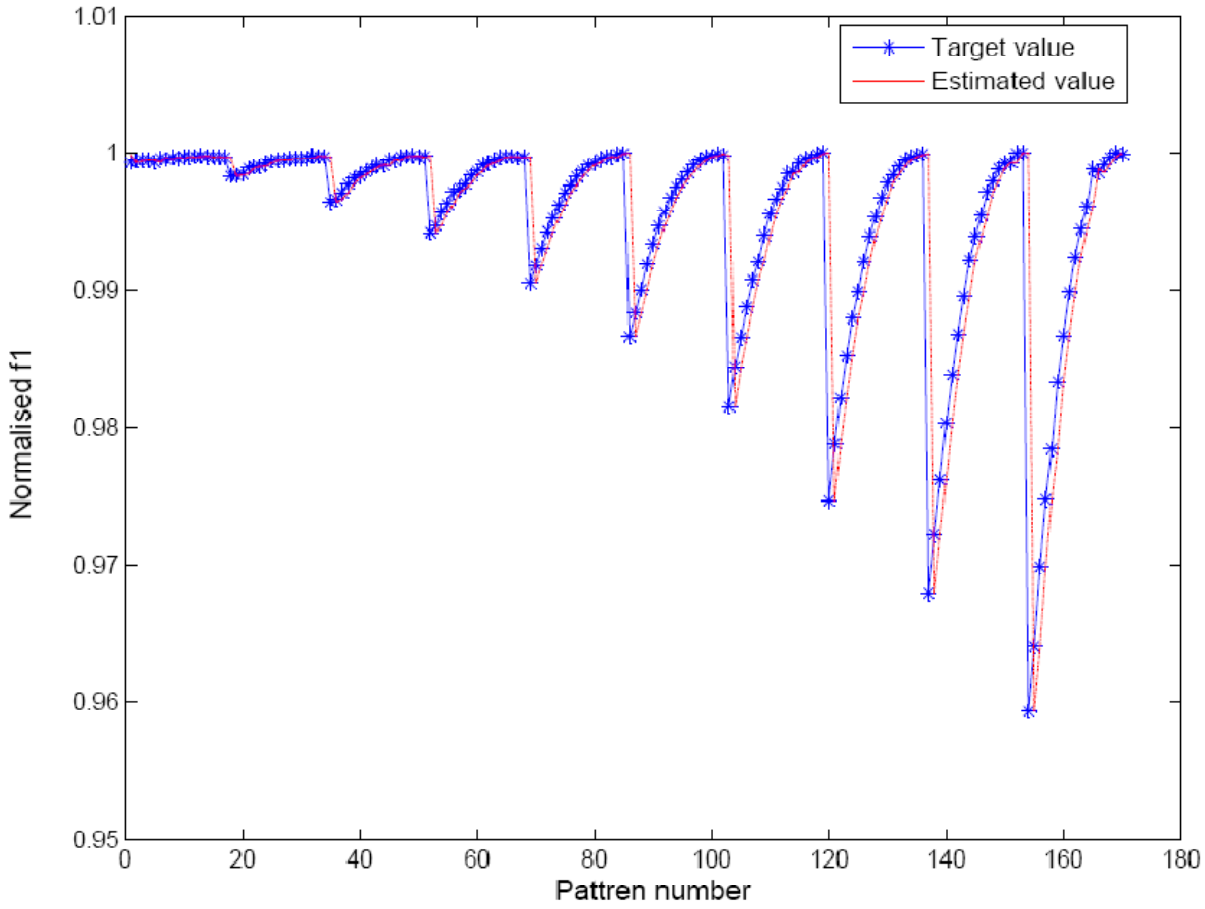

Fig.6.3.1. Comparison of the first estimated eigenfrequencies from the neural network to target values:

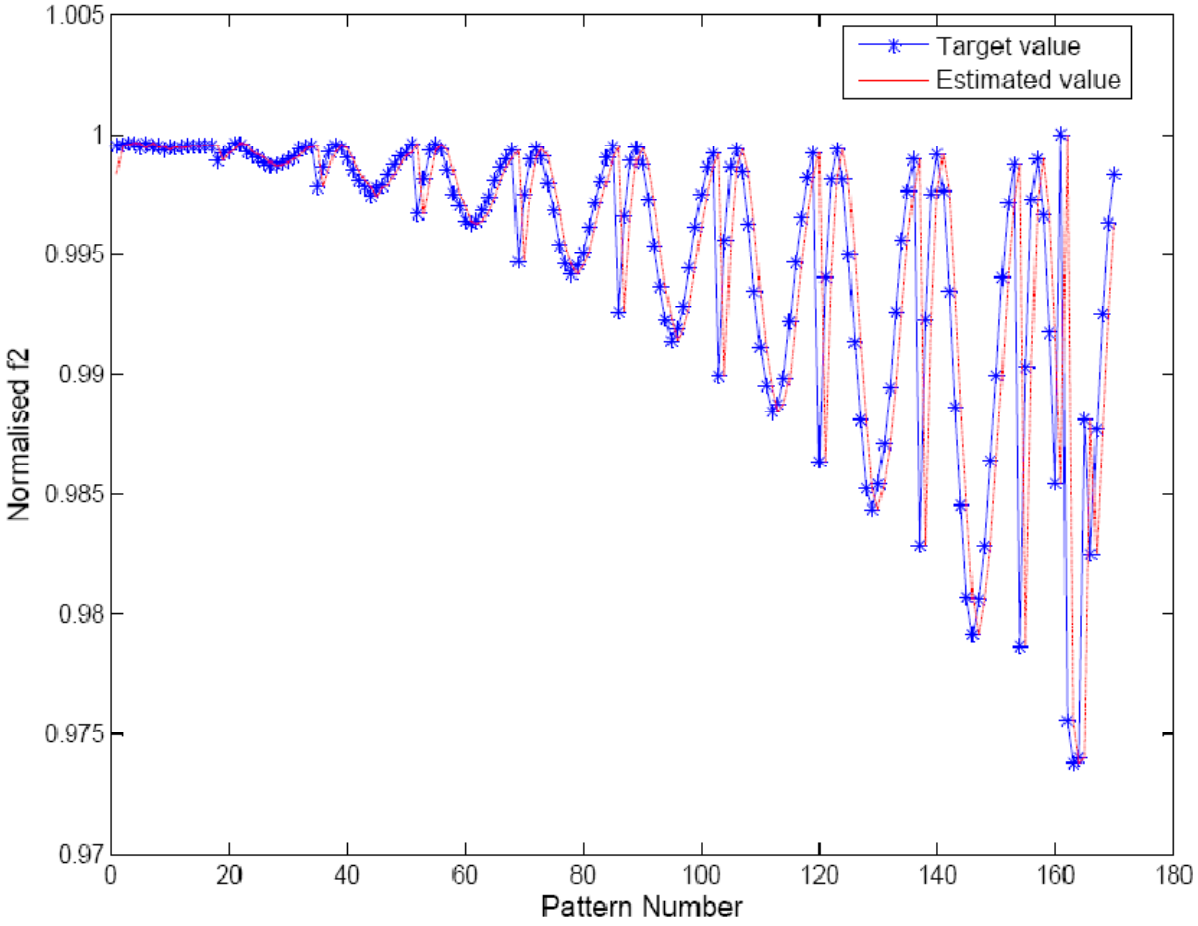

Fig.6.3.2. Comparison of the Second estimated eigenfrequencies from the neural network to target values:

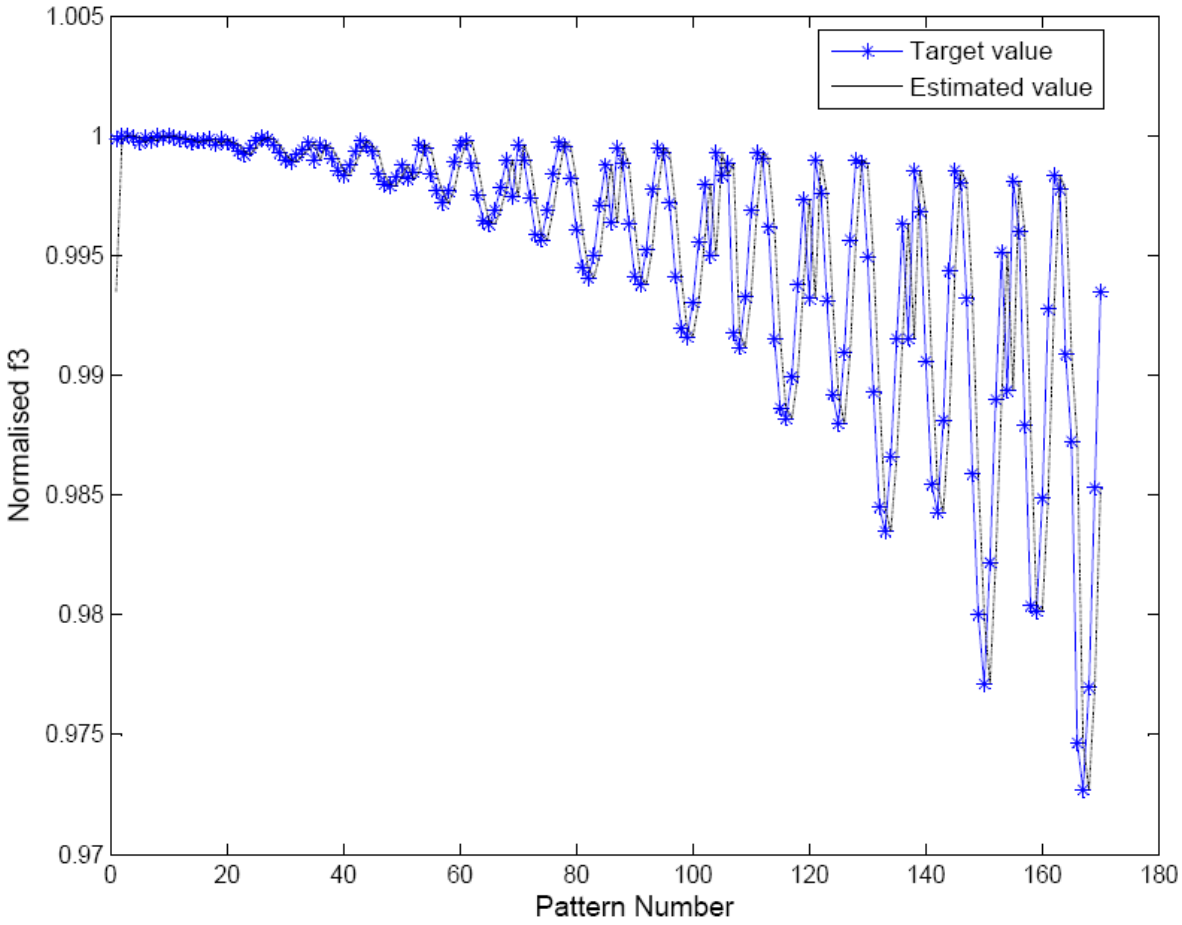

Fig.6.3.3.Comparison of the third estimated eigenfrequencies from the neural network to target values:

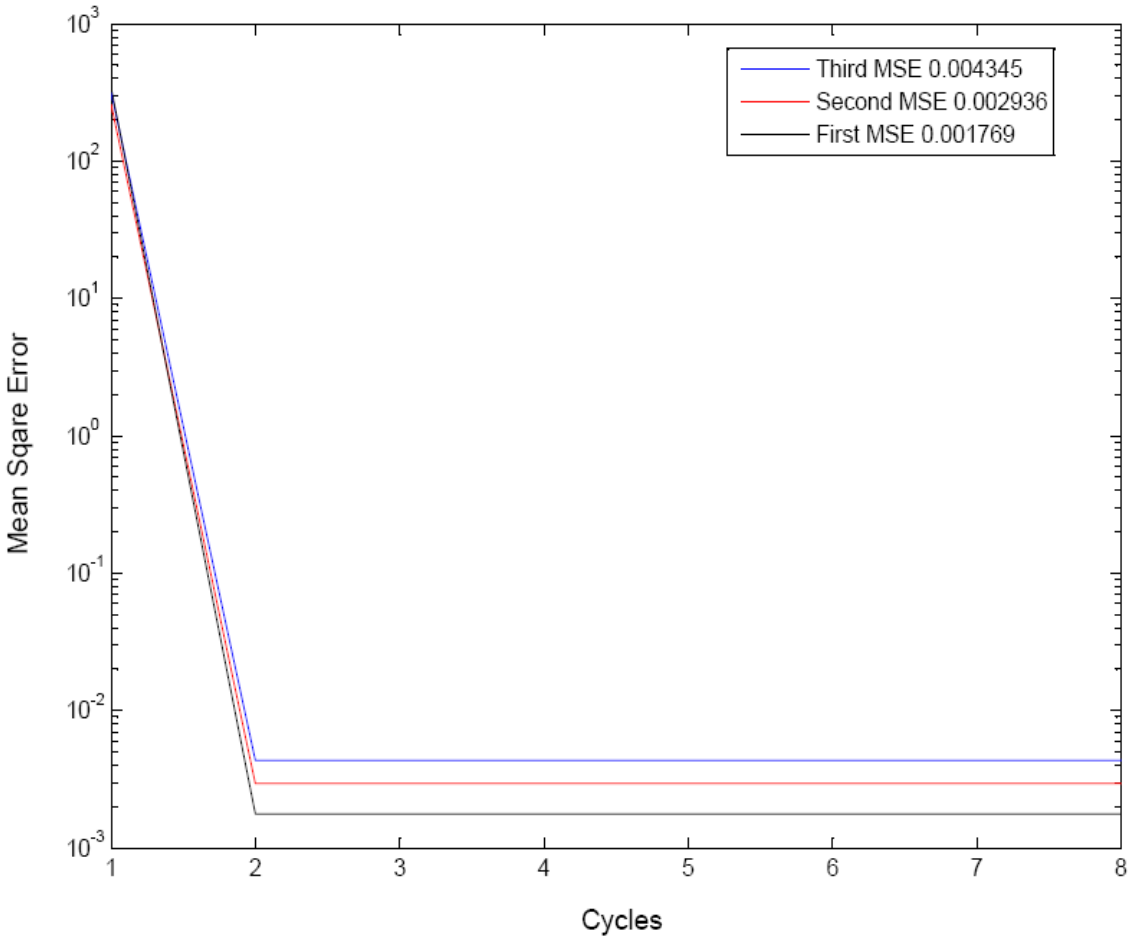

Fig.6.3.4. Neural network output.

6.4 DISCUSSION

The first, second and third natural frequencies corresponding to various crack locations and depths are calculated. The fundamental mode shapes for transverse vibration of cracked and uncracked beams are plotted and compared. The results obtained from the numerical analysis are presented in graphical form. Results show that there is an appreciable variation between natural frequency of cracked and uncracked cantilever beam. With increase in mode of vibration this difference increases.

The transverse vibration mode shapes for two crack aluminium beam are shown in fig.6.1-6.9.In these figures different combinations of crack depths ($a_1/w=a_2/w=0.1667,0.334$, 0.5) are considered. The relative crack locations are chosen at 0.125 and 0.25. For moderate cracks appreciable changes in mode shapes are noticed and for deep cracks the changes in mode shapes are quite substantial. However remarkable changes are observed in longitudinal mode shapes at the crack positions. The longitudinal mode shapes for two cracks as shown in fig.6.10-6.15. The numerical results indicate that the deviation between the fundamental mode shapes of the cracked and uncracked beam is always sharply changed at the crack location. The simulation results obtained by ANSYS software are shown in Figs. 6.21-6.26.

The three-layer neural network having an input layer (I) with four input nodes, a hidden layer (H) with thirteen neurons and an output layer (O) with four output node employed for this work is shown in Fig.5.5.The estimated eigenfrequencies from the network are compared to the target values as shown in Figure 6.3.1-6.3.4. The target values are f_1*, f_2* and f_3* in Figure 5.5 which are the reference data or training data to have trained the neural network. One hundred and seventy patterns are arranged in 10 separate curves base on the value of a as shown in the Figure. In Fig.6.3.1 shows the first eigenfrequency f_1 is monotonously increasing as the crack location moves from the clamped end to the free end when the crack depth $a_1=a_2$ is kept constant. On the other hand, the second and the third eigenfrequencies oscillate under the same situation as shown in Fig.6.3.2 and 6.3.3.

Mean-square error (MSE) is employed as a measurement of modelling performance. As shown in figure 6.3.4 the first MSE is 0.001769, second MSE is 0.002936 and third MSE is 0.004345.

CHAPTER 7

CONCLUSION AND SCOPE FOR FUTURE WORK

7. CONCLUSION AND SCOPE FOR FUTURE WORK

The presence of crack in structure member introduces local flexibilities which can be computed and used in structural analysis. Analytical computational method can be used for solving the frequency of equation of elastic beam with cracks. It is shown that the natural frequency changes substantially due to the presence of cracks. The changes depending upon the location and size of cracks. The position of the cracks can be predicted from the deviation of the fundamental modes between the cracked and uncracked beam.

The frequency of the cracked cantilever beam decreases with increase in the crack depth for the all modes of vibration. For moderate cracks ($a_1/w=a_2/w=0.1667$) appreciable changes in mode shapes are noticed and for deep cracks ($a_1/w=a_2/w=0.5$) the change in mode shapes are quite substantial.

Feed-forward multi-layer neural networks trained by back-propagation are used to learn the input (the location and depth of a crack)-output (the structural eigenfrequencies) relation of the structural system. From neural network training, the first eigenfrequency f_1 is monotonously increasing as the crack location moves from the clamped end to the free end when the crack depth $a_1=a_2$ is kept constant. On the other hand, the second and the third eigenfrequencies oscillate under the same situation. The first MSE is 0.001769, second MSE is 0.002936 and third MSE is 0.004345. A neural network for the cracked structure is trained to approximate the response of the structure by the data set prepared for various crack sizes and locations. Training data to train the neural network are properly prepared.

FUTURE WORK

- The cracked cantilever can be analyzed under the influence of external forces.
- The dynamic response of the cracked beams can be analyzed for different crack orientations.
- Stability study of the cracked beams can be done.
- Use hybrid neuro genetic technique for crack detection.

CHAPTER 8

REFERENCES

8. REFERENCES

1. Orhan Sadettin, Analysis of free and forced vibration of a cracked cantilever beam, NDT and E International 40, (2007), pp.43-450.
2. Chasalevris Athanasios C. and Papadopoulos Chris A., Identification of multiple cracks in beams under bending, Mechanical Systems and Signal Processing 20, (2006), pp.1631-1673.
3. Nahvi H. and Jabbari M., Crack detection in beams using experimental modal data and finite element model, International Journal of Mechanical Sciences 47, (2005), pp.1477–1497.
4. Yang X. F., Swamidas A. S. J. and Seshadri R., Crack Identification in vibrating beams using the Energy Method, Journal of Sound and vibration 244(2), (2001), pp.339-357.
5. Dharmaraju N., Tiwari R. and Talukdar S., Identification of an open crack model in a beam based on force–response measurements, Computers and Structures 82, (2004), pp.167–179.
6. Ruotolo R, et al. Harmonic analysis of the vibrations of a cantilevered beam with a closing crack, Comput Struct, 61(6), (1996), pp.1057–1074.
7. Patil D.P., Maiti S.K., Experimental verification of a method of detection of multiple cracks in beams based on frequency measurements, Journal of Sound and Vibration 281,(2005), pp.439–451.
8. Patil D.P., Maiti S.K, Detection of multiple cracks using frequency measurements, Engineering Fracture Mechanics 70, (2003), pp.1553–1572.
9. Kisa Murat and Gurel M. Arif, Free vibration analysis of uniform and stepped cracked beams with circular cross sections, International Journal of Engineering Science 45, (2007), pp.364–380.
10. Kisa M. and Brandon J., The Effects of closure of cracks on the dynamics of a cracked cantilever beam, Journal of Sound and Vibration, 238(1), (2000) pp.1-18
11. Loutridis S., Douka E. and Hadjileontiadis L.J., Forced vibration behaviour and crack detection of cracked beams using instantaneous frequency, NDT&E International, 38(5), (2005), pp. 411-419.

12. Darpe A.K.,Gupta K., Chawla A., Dynamics of a two-crack rotor, Journal of Sound and Vibration, 259 (3), (2003), pp.649–675.
13. Ertuğrul Çam, Orhan Sadettin and Lüy Murat , An analysis of cracked beam structure using impact echo method, NDT and E International 38, (2005), pp.368–373.
14. Fang X., Luo H. and Tang J., Structural damage detection using neural network with learning rate improvement, Computers and Structures 83 (2005), pp. 2150–2161.
15. Suh M.W., Shim M. B. and Kim M. Y. Crack Identification using hybrid neuro – genetic technique, Journal of Sound and vibration 238(4), (2000), pp.617-635.
16. Chondros T.G, Dimarogonas A.D and Yao, J. A. continuos cracked beam vibration theory, Journal of Sound and Vibration, 215, (1998), pp.17-34.
17. Rizos P.F., Aspragathos N., and Dimarogonas A.D., Identification of cracked location and magnitude in a cantilever beam from the vibrational modes, Journal of Sound and Vibration, 138 (3), (1989), pp.381 – 388.
18. Baris Binici, Vibration of beams with multiple open cracks subjected to axial force, Journal of Sound and Vibration 287, (2005), pp.277–295.
19. Sekhar A.S., Mohanty A.R. and Prabhakar S., Vibrations of cracked rotor system: transverse crack versus slant crack, Journal of Sound and Vibration 279, (2005), pp. 1203–1217.
20. Sekhar A.S., Model based identification of two cracks in a rotor system, Mechanical Systems and Signal Processing, 18, (2004), pp.977–983.
21. Suresh S, Omkar S. N., Ganguli Ranjan and Mani V, Identification of crack location and depth in a cantilever beam using a modular neural network approach, Smart Materials and Structures, 13, (2004) pp.907-915.
22. Tsai T. C. and Wang Y. Z., Vibration Analysis and diagnosis of a cracked beam, Journal of Sound and Vibration,192(3), (1996)pp.607-620.
23. Zheng D.Y., Kessissoglou N.J., Free vibration analysis of a cracked beam by finite element method, Journal of Sound and Vibration 273, (2004) pp.457–475.
24. Hwang H.Y.,Kim C., Damage detection in structures using a few frequency response, Journal of Sound and Vibration 270, (2004), pp. 1–14.

25. Fernandez-saez J., Rubio L. and Navarro C., Approximate calculation of the fundamental frequency for bending vibrations of cracked beams. Journal of Sound and Vibration 225 (2), (2002), pp. 345-352.
26. Chandra Kishen, J.M., and Kumar, A., Finite element analysis for fracture behavior of cracked beam-columns, Finite Elements in Analysis and Design, 40,(2004), pp.1773 – 1789.
27. Sahin M , Shenoi R.A., Quantification and localisation of damage in beam-like structures by using artificial neural networks with experimental validation, Engineering Structures, 25, (2003), pp.1785–1802.
28. Douka E., Bamnios G., Trochidis A., A method for determining the location and depth of cracks in double-cracked beams, Applied Acoustics, 65, (2004), pp. 997–1008.
29. Han-Ik Yoona, In-Soo Sona, Sung-Jin Ahn, Free Vibration Analysis of Euler-Bernoulli beam with double Cracks, Journal of Mechanical Science and Technology, 21, (2007), pp. 476-485.
30. Gounaris George, Papadopoulos Chris A. Crack identification in rotating shafts by coupled response measurements Engineering Fracture Mechanics, 69, (2002), pp.339-352.
31. Behera R.K., Vibration Analysis of multi cracked structure, PhD Thesis.
32. Tada H, Paris P.C. and Irwin G.R, The stress analysis of cracks Handbook, Third edition- ASME PRESS, 2000.
33. Stephan H.C., Norman C.D. and Thoms J.L. An Introduction of mechanics of solids, McGraw Hill book company, Second edition, 1978.
34. Rajsekaran S, Vijayalakshmi Pai G. A., Neural network, fuzzy logic & genetic algorithm synthesis and application, Pentice Hall.
35. Haykin S. "Neural Networks: A comprehensive Foundation", Pearson Edition Asia, 2002.
36. Madenci Erdogan, Guven Ibrahim, The Finite Element Method Application in Engg. by using ANSYS, (Springer)2007.
37. Inman Daniel J., Engineering vibration Third edition, Pearson Pentice Hall (2007).
38. Singiresu S. Rao, Mechanical vibrations, Pearson education (2007).
39. Bavikatti S., Finite Element Analysis, New Age International (p) Ltd.